

# Local fluctuations in quantum critical metals

Qimiao Si\*, Silvio Rabello\*, Kevin Ingersent†, and J. Llewellyn Smith\*

\**Department of Physics & Astronomy, Rice University, Houston, TX 77251-1892, U.S.A.*

†*Department of Physics, University of Florida, Gainesville, FL 32611-8440, U.S.A.*

We show that spatially local, yet low-energy, fluctuations can play an essential role in the physics of strongly correlated electron systems tuned to a quantum critical point. A detailed microscopic analysis of the Kondo lattice model is carried out within an extended dynamical mean-field approach. The correlation functions for the lattice model are calculated through a self-consistent Bose-Fermi Kondo problem, in which a local moment is coupled both to a fermionic bath and to a bosonic bath (a fluctuating magnetic field). A renormalization-group treatment of this impurity problem—perturbative in  $\epsilon = 1 - \gamma$ , where  $\gamma$  is an exponent characterizing the spectrum of the bosonic bath—shows that competition between the two couplings can drive the local-moment fluctuations critical. As a result, two distinct types of quantum critical point emerge in the Kondo lattice, one being of the usual spin-density-wave type, the other “locally critical.” Near the locally critical point, the dynamical spin susceptibility exhibits  $\omega/T$  scaling with a fractional exponent. While the spin-density-wave critical point is Gaussian, the locally critical point is an interacting fixed point at which long-wavelength and spatially local critical modes coexist. A Ginzburg-Landau description for the locally critical point is discussed. It is argued that these results are robust, that local criticality provides a natural description of the quantum critical behavior seen in a number of heavy-fermion metals, and that this picture may also be relevant to other strongly correlated metals.

PACS numbers: 71.10.Hf, 71.27.+a, 75.20.Hr, 71.28.+d

## I. INTRODUCTION

Non-Fermi-liquid properties have been seen experimentally in a number of strongly correlated electron systems.<sup>1–3</sup> They pose fundamental questions about how electron correlations lead to new electronic states of matter and new elementary excitations. One mechanism for the breakdown of Fermi-liquid theory is quantum criticality. While the extent to which an underlying quantum critical point (QCP) plays a role in the non-Fermi-liquid behavior of high-temperature superconductors remains a subject of debate,<sup>4</sup> the situation is much clearer in heavy-fermion metals. Among the many heavy-fermion materials in which non-Fermi-liquid properties have been seen,<sup>1,5–15</sup> magnetic QCPs have been explicitly identified in a number of stoichiometric or nearly stoichiometric materials<sup>5–8</sup> including  $\text{CeCu}_{6-x}\text{Au}_x$ ,  $\text{CePd}_2\text{Si}_2$ ,  $\text{CeIn}_3$ , and  $\text{YbRh}_2\text{Si}_2$ . In each of these systems, the zero-temperature magnetic ordering transition appears to be continuous. Non-Fermi-liquid behavior, usually seen in the temperature dependences of transport and thermodynamic properties, arises near the QCP. For instance, the resistivity is linear (or close to being linear) in  $T$ , and the temperature dependence of the specific heat coefficient  $C/T$  is either logarithmically singular or nonanalytic with a finite zero-temperature limit. Away from the quantum critical regime, there is a gradual recovery of Fermi-liquid behavior (albeit still with a large effective mass). These materials provide controlled settings in which to study not only basic issues concerning magnetism in heavy fermions, but also the physics of QCPs in strongly correlated metals in general.

Inelastic neutron scattering directly probes the critical fluctuations at heavy-fermion magnetic QCPs. Partic-

ularly detailed measurements have been performed on  $\text{CeCu}_{6-x}\text{Au}_x$ , which can be tuned from a paramagnetic metal to an antiferromagnetic metal by varying  $x$  and/or an applied pressure. The results<sup>16–19</sup> are striking in a number of ways: (1) The frequency dependence of the dynamical spin susceptibility displays a fractional exponent. (2) The same exponent also appears in the temperature dependence; the dynamical spin susceptibility has  $\omega/T$  scaling. (3) This fractional exponent describes the variation with frequency and temperature not only at the ordering wavevector, but essentially everywhere else in the Brillouin zone.

The existence of the fractional exponent is a surprise. It is standard to assume<sup>20–25</sup> that the critical theory for magnetic QCPs in metals is a  $\phi^4$  theory, describing the long-wavelength fluctuations of the magnetic order parameter. Landau damping makes the dynamic exponent  $z$  larger than 1. In the antiferromagnetic case,  $z = 2$ , so the effective dimensionality of the  $\phi^4$  theory,  $d_{\text{eff}} = d + z$ , is greater than (equal to) its upper critical dimension for spatial dimensionality  $d = 3$  ( $d = 2$ ). Consequently, in the standard picture all the nonlinear couplings are irrelevant in the renormalization-group (RG) sense, the fixed point is Gaussian, and the frequency exponent must take its mean-field value of 1.

Likewise, the existence of  $\omega/T$  scaling is surprising. For a Gaussian fixed point, the spin relaxation rate is determined by nonlinear couplings that are irrelevant in the RG sense. This implies that the relaxation rate is superlinear in temperature,<sup>26</sup> whereas  $\omega/T$  scaling can arise only for a linear relaxation rate.

Both of these features, then, imply that the critical point in  $\text{CeCu}_{6-x}\text{Au}_x$  has to be an interacting one. What is the new physics that is responsible for the interact-

ing part of the critical theory? A clue is provided by the third feature of the experimental data mentioned above. The fact that the fractional exponent in the frequency/temperature dependence occurs also at generic wavevectors (far away from the ordering wavevector) suggests that the origin of the fractional exponent lies in some type of local physics.<sup>17</sup>

Heavy-fermion metals undergoing a magnetic quantum phase transition should be well-described by the Kondo lattice model of local moments interacting with conduction-band electrons. It is natural, therefore, to suspect that the local physics responsible for the anomalous properties of  $\text{CeCu}_{6-x}\text{Au}_x$  involves the magnetic moments. In Ref. 27, we briefly reported an interacting critical point in Kondo lattice systems. (See also Ref. 28 for more qualitative discussions.) Our analysis was carried out using an extended dynamical mean field theory (EDMFT), supplemented by Ginzburg-Landau considerations. Other approaches, based on a large- $N$  formulation, have also been developed to study this problem,<sup>29,30</sup> although they have yet to yield any new type of QCPs. A scenario of three-dimensional electrons coupled to two-dimensional Gaussian spin fluctuations<sup>19,31,6</sup> has also been proposed, but it does not address the local and other non-Gaussian aspects of the critical dynamics.

The present paper describes in detail our microscopic analysis of the Kondo lattice. The interplay of local and spatially extended physics is treated using the EDMFT developed in Refs. 32–34. The central result is the finding of two types of quantum phase transition. The first, corresponding to the Gaussian picture, describes a transition of the usual spin-density-wave (SDW) type, and is found to occur when the underlying spin fluctuations are three-dimensional in character. We dub the other type of transition “locally critical,” because long-wavelength and spatially local critical modes coexist at the QCP. This type of transition occurs if the spin fluctuations are (quasi-)two-dimensional. Near the locally critical point, the dynamical spin susceptibility exhibits  $\omega/T$  scaling with a fractional exponent. By analyzing the general form of the interacting critical theory, we argue that the existence of two types of critical point is valid beyond the approximations contained in our microscopic calculations. The locally critical picture provides a natural description of the quantum critical behavior seen in a number of heavy-fermion metals, and is argued to be of importance in the broader context of strongly correlated electron physics.

The remainder of the paper is organized as follows. We introduce the model and its EDMFT formulation in Section II. The EDMFT equations have the content of a Bose-Fermi Kondo model supplemented by self-consistency conditions. In Section III, we present a detailed RG analysis of the Bose-Fermi Kondo model, when the bath spectral functions are assumed to take power-law forms. A critical point is identified in the impurity model, and the spin correlation functions near this critical point are calculated. Using this solution to the impu-

rity model, we study in Section IV the self-consistent EDMFT problem. Two types of QCP are identified, and their zero-temperature dynamics are determined. The finite-temperature spin dynamics are studied in Section V. A Ginzburg-Landau analysis is presented in Section VI. Section VII compares our theoretical results with experiments in heavy-fermion systems. Section VIII contains concluding remarks and discusses the general relevance of critical local physics. Details of the derivation of the RG equations, of the determination of the separatrix between the two stable phases of the Bose-Fermi Kondo model, and of the calculation of correlation functions at the critical point of the impurity model are given in Appendices A, B, and C, respectively. Finally, Appendix D presents the derivation of correlation functions for the long-ranged one-dimensional spherical model with an interaction that decays with distance either as a pure power-law or with logarithmic corrections.

## II. THE MODEL AND FORMALISM

### A. Kondo Lattice Model

The Kondo lattice model is specified by the Hamiltonian

$$\mathcal{H} = \sum_{ij\sigma} t_{ij} c_{i\sigma}^\dagger c_{j\sigma} + \sum_i J_K \mathbf{S}_i \cdot \mathbf{s}_{c,i} + \sum_{ij} \frac{I_{ij}}{2} \mathbf{S}_i \cdot \mathbf{S}_j. \quad (1)$$

At each lattice site  $i$  is located a spin- $\frac{1}{2}$  local moment  $\mathbf{S}_i$ , which interacts on-site with the spin  $\mathbf{s}_{c,i}$  of the conduction ( $c$ ) electrons. The tight-binding parameters  $t_{ij}$  determine the dispersion  $\epsilon_{\mathbf{k}}$  and, hence, the bare conduction-band density of states

$$\rho_0(\epsilon) = \sum_{\mathbf{k}} \delta(\epsilon - \epsilon_{\mathbf{k}}). \quad (2)$$

We will treat only cases where the average number of conduction electrons is less than one per site. All the phases described below are metallic.

Two processes oppose each other in the Kondo lattice. First, each magnetic moment couples locally with strength  $J_K$  to the spins of the conduction electrons. We consider only positive (antiferromagnetic)  $J_K$  values, which can lead to Kondo-quenching of the local moments. Second, the magnetic moments interact with each other through the nonlocal, RKKY coupling  $I_{ij}$ . In Eq. (1), we have introduced an explicit RKKY interaction term in addition to that induced implicitly by the Kondo coupling  $J_K$ . This is done so that the dynamics associated with the RKKY interactions can be incorporated into the EDMFT.<sup>32–34</sup> (The EDMFT ensures that there is no double-counting of the implicit and explicit RKKY interactions.<sup>32</sup>) For the systems under consideration,  $I_{\mathbf{q}}$ , the spatial Fourier transform of  $I_{ij}$ , is most negative when  $\mathbf{q}$  is equal to the antiferromagnetic wavevector,  $\mathbf{Q} \neq \mathbf{0}$ .

The competition between the Kondo effect and the RKKY interaction is expected to lead to a magnetic quantum phase transition.<sup>35,36</sup> Traditionally, it is assumed that the local moments are quenched, not only on the paramagnetic side but also through the transition. In this picture, the quantum phase transition corresponds to an SDW instability of heavy quasiparticles produced by the quenching, and the quantum critical behavior is necessarily that of a Gaussian fixed point. By contrast, our analysis makes no prior assumption that Kondo resonances are fully developed. It should be stressed—as a discussion at the end of Section IV A will make clear—that the critical point is always reached by tuning just one parameter: the ratio of the effective RKKY interaction and an effective Kondo coupling.

### B. Extended dynamical mean field theory

In the EDMFT,<sup>32–34</sup> all the correlation functions of the Kondo lattice can be calculated in terms of a self-consistent Kondo impurity model. The EDMFT generalizes the standard dynamical mean-field theory<sup>37</sup> in that it incorporates the quantum fluctuations produced by any intersite interaction; in the Kondo lattice model (1) this is the RKKY interaction. A key quantity introduced in the EDMFT is the “spin self-energy”  $M(\omega)$ , in terms of which the momentum-dependent dynamical spin susceptibility can be written

$$\chi(\mathbf{q}, \omega) = \frac{1}{M(\omega) + I_{\mathbf{q}}}. \quad (3)$$

(More specifically, the spin self-energy is defined in terms of an effective spin cumulant that is  $I$ -irreducible.<sup>32</sup>) The conduction-electron Green’s function is, as usual, expressed in terms of the conduction-electron self-energy  $\Sigma(\omega)$ :

$$G(\mathbf{k}, \omega) = \frac{1}{\omega + \mu - \epsilon_{\mathbf{k}} - \Sigma(\omega)}. \quad (4)$$

A crucial advantage of the EDMFT is that, unlike standard RPA approximations, the damping of spin fluctuations is not restricted to take place via decay into quasiparticle-quasihole pairs. Instead the (dynamical) solution of the problem will dictate the nature of the low-energy many-body excitations and the associated form of the spin damping. At the same time, it is important to bear in mind the central approximation made in the EDMFT, namely, both  $\Sigma$  and  $M$  are taken to be momentum-independent.

Details of the formalism have been published in Ref. 32. Here we stress that the EDMFT can be adopted as a conserving resummation of diagrams for finite-dimensional systems. As discussed in Ref. 32, the diagrams retained in the EDMFT form an infinite series, which is illustrated in Fig. 1. (Note that standard Feynman diagrams can be used for the Kondo lattice model

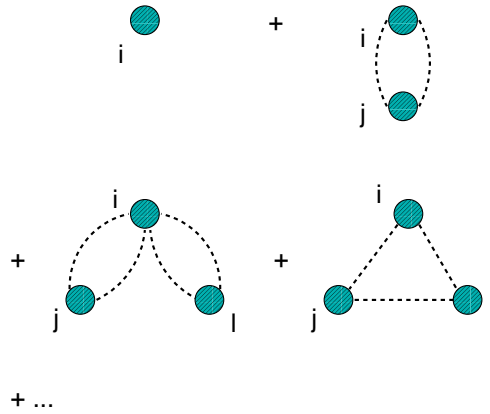


FIG. 1. Single-site, two-site, and three-site diagrams for the Luttinger-Ward potential in the extended dynamical mean-field theory. A dashed line represents an intersite interaction; this is  $I_{ij}$  for the Hamiltonian given in Eq. (1). A blob contains all the on-site diagrams, with the associated (fully dressed) fermion Green’s function. The series extends to diagrams involving an infinite number of sites.

once the spin of the local moment is represented in terms of pseudo-fermions without a constraint; one such representation suitable for the spin- $\frac{1}{2}$  case we are considering is the Popov representation.<sup>38</sup>)

The spatial dimensionality  $d$  and other aspects of the lattice structure are encoded in the form of the tight-binding parameter  $t_{ij}$  and the RKKY interaction  $I_{ij}$ . In particular, a quantity that will play a crucial role in our analysis is the “RKKY density of states,”

$$\rho_I(\epsilon) \equiv \sum_{\mathbf{q}} \delta(\epsilon - I_{\mathbf{q}}). \quad (5)$$

For any finite-dimensional system,  $I_{\mathbf{q}}$  is nonzero only over a finite range. In other words, the support of  $\rho_I(\epsilon)$  is bounded. This ensures that there is a finite region of parameter space over which  $\chi(\mathbf{q}, \omega)$  is positive and non-singular; hence, a stable paramagnetic solution exists. An alternative construction of the EDMFT, also given in Ref. 32, scales the intersite parameters such that the nearest-neighbor coupling goes as  $I_{(ij)} \propto 1/\sqrt{d}$ , and then takes the limit  $d \rightarrow \infty$ . In this case, a special choice of lattice has to be made in order to obtain a stable paramagnetic solution.

### C. Extended dynamical mean-field equations for the Kondo lattice

The EDMFT equations for the Kondo lattice model can be expressed in terms of an effective action for a single lattice site (the “impurity” site):

$$\mathcal{S}_{\text{imp}} = \mathcal{S}_{\text{top}} + \int_0^\beta d\tau J_K \mathbf{S} \cdot \mathbf{s}_c$$

$$\begin{aligned}
& - \int_0^\beta d\tau \int_0^\beta d\tau' \left[ \sum_\sigma c_\sigma^\dagger(\tau) G_0^{-1}(\tau - \tau') c_\sigma(\tau') \right. \\
& \left. + \frac{1}{2} \mathbf{S}(\tau) \cdot \chi_0^{-1}(\tau - \tau') \mathbf{S}(\tau') \right], \quad (6)
\end{aligned}$$

where  $\beta = 1/k_B T$ ,  $\mathcal{S}_{\text{top}}$  describes the Berry phase of the local moment, and  $G_0^{-1}$  and  $\chi_0^{-1}$  are Weiss fields.

Equivalently, the effective impurity action can be represented in terms of the following effective impurity Hamiltonian:

$$\begin{aligned}
\mathcal{H}_{\text{imp}} = & J_K \mathbf{S} \cdot \mathbf{s}_c + \sum_{p,\sigma} E_p c_{p\sigma}^\dagger c_{p\sigma} \\
& + g \sum_p \mathbf{S} \cdot \left( \vec{\phi}_p + \vec{\phi}_{-p}^\dagger \right) + \sum_p w_p \vec{\phi}_p^\dagger \cdot \vec{\phi}_p. \quad (7)
\end{aligned}$$

This is the Bose-Fermi Kondo Hamiltonian, describing a local moment coupled not only to the spin of a fermionic bath ( $c_{p\sigma}$ ), as in the usual Kondo problem, but also to a dissipative vector-bosonic bath ( $\vec{\phi}_p$ ). Physically, the vector bosons describe a fluctuating magnetic field generated via the RKKY interaction by the local moments at all other lattice sites. The dispersions,  $E_p$  and  $w_p$ , as well as the coupling constant  $g$ , are such that integrating out the two baths in the Hamiltonian representation yields the effective action (6). Specifically,

$$\begin{aligned}
g^2 \sum_p \frac{2w_p}{(i\nu_m)^2 - w_p^2} &= -\chi_0^{-1}(i\nu_m), \\
\sum_p \frac{1}{i\omega_n - E_p} &= G_0(i\omega_n), \quad (8)
\end{aligned}$$

where  $\nu_m$  and  $\omega_n$  are bosonic and fermionic Matsubara frequencies, respectively. In the following, we will interchange between the two representations based on notational convenience.

The self-consistent procedure goes as follows:

1. Put in trial forms for  $\chi_0^{-1}(i\nu_m)$  and  $G_0^{-1}(i\omega_n)$ .
2. Solve the impurity Kondo problem to determine the impurity correlation functions,

$$\chi_{\text{imp}}(\tau) \equiv \langle T_\tau S^x(\tau) S^x(0) \rangle \quad (9)$$

and

$$G_{\text{imp}}(\tau) \equiv -\langle T_\tau c_\sigma(\tau) c_\sigma^\dagger(0) \rangle. \quad (10)$$

This step also determines the spin self-energy through a Dyson-like equation for the impurity problem,

$$M_{\text{imp}}(i\nu_m) = \chi_0^{-1}(i\nu_m) + \frac{1}{\chi_{\text{imp}}(i\nu_m)}, \quad (11)$$

and a conduction-electron self-energy,

$$\Sigma_{\text{imp}}(i\omega_n) = G_0^{-1}(i\omega_n) - \frac{1}{G_{\text{imp}}(i\omega_n)}. \quad (12)$$

3. Determine the parameters in the trial forms of  $\chi_0^{-1}(i\nu_m)$  and  $G_0^{-1}(i\omega_n)$  by demanding self-consistency. The self-consistency conditions

$$\begin{aligned}
\chi_{\text{imp}}(\omega) &= \sum_{\mathbf{q}} \chi(\mathbf{q}, \omega), \\
G_{\text{imp}}(\omega) &= \sum_{\mathbf{k}} G(\mathbf{k}, \omega), \quad (13)
\end{aligned}$$

amount to the requirement that each local correlation function is equal to the wave-vector average of the corresponding lattice correlation function. The lattice spin susceptibility and lattice Green's function,  $\chi(\mathbf{q}, i\nu_m)$  and  $G(\mathbf{k}, i\omega_n)$ , respectively, are given in Eqs. (3) and (4).

4. Once self-consistency is achieved, identify the impurity quantities  $\chi_{\text{imp}}$  and  $G_{\text{imp}}$  with the corresponding local (on-site) quantities  $\chi_{\text{loc}}$  and  $G_{\text{loc}}$  of the lattice problem. Likewise, identify  $M_{\text{imp}}$  and  $\Sigma_{\text{imp}}$  with the corresponding lattice quantities  $M$  and  $\Sigma$ , and hence use Eqs. (3) and (4) to calculate the lattice dynamical spin susceptibility  $\chi(\mathbf{q}, i\nu_m)$  and the lattice Green function  $G(\mathbf{k}, i\omega_n)$ .

The derivation of Eqs. (3), (4), and (11) has been given in Ref. 32. For notational simplicity, in the remainder of the paper we will not differentiate between impurity quantities and local quantities. In particular, the impurity spin-spin correlation function determined from the Bose-Fermi Kondo model will simply be called  $\chi_{\text{loc}}$ .

### III. SOLUTION OF THE IMPURITY PROBLEM

Our goal is to determine the universal low-energy behavior of the effective impurity problem generated by the EDMFT. For this purpose, we choose trial forms for the Weiss fields such that the density of states of the fermion bath near the Fermi energy is a nonzero constant,

$$\sum_p \delta(\omega - E_p) = N_0, \quad (14)$$

while the spectral function of the fluctuating magnetic field has a sublinear power-law dependence on energy at sufficiently low energies:

$$\sum_p \delta(\omega - w_p) = (K_0^2/\pi) |\omega|^\gamma \quad \text{for } |\omega| < \Lambda, \quad (15)$$

with  $\gamma < 1$ . Equivalently—through Eq. (8)—the imaginary part of the Weiss field takes the form

$$\text{Im } \chi_0^{-1}(\omega + i0^+) = C |\omega|^\gamma \text{sgn } \omega, \quad (16)$$

where

$$C = (K_0 g)^2. \quad (17)$$

Eq. (15) also defines the cutoff parameter  $\Lambda$ . The self-consistency of our trial forms for the Weiss fields will be established in Section IV, where the solution for  $\gamma$ ,  $C$ ,  $\Lambda$ , and  $N_0$  will also be given.

Having specified the parameters of the impurity model, we now proceed to solve this model. Our strategy is first to construct the RG equations for the coupling constants  $J_K$  and  $g$ . We then show that a phase transition exists as the ratio  $g/T_K^0$  is varied. [Here we parametrize the Kondo coupling  $J_K$  using the single-impurity Kondo temperature,

$$T_K^0 \approx \frac{1}{\rho_0(\mu)} e^{-1/\rho_0(\mu)J_K}, \quad (18)$$

where  $\rho_0(\mu)$  is the bare conduction-electron density of states at the chemical potential  $\mu$ .] The critical value of  $g/T_K^0$  is determined to linear order in  $1-\gamma$ . We then calculate the correlation functions at the critical point, also to linear order in  $1-\gamma$ . This  $(1-\gamma)$ -expansion was first introduced to the Bose-Fermi Kondo model by Smith and Si<sup>39</sup> [following an earlier  $(1-\gamma)$ -expansion for a spinless Bose-Fermi Kondo model<sup>33</sup>] and by Sengupta.<sup>40</sup> It was subsequently used to study a Bose Kondo model with an interacting bath by Vojta, Buragohain, and Sachdev.<sup>41</sup>

Both the construction of the RG equations and the calculation of correlation functions require a proper handling of the spin operators. Following Smith and Si,<sup>39</sup> we adopt the Abrikosov representation of the spin in terms of pseudo- $f$ -electrons,<sup>42</sup>

$$\mathbf{S} = \sum_{\sigma\sigma'} f_{\sigma}^{\dagger} \frac{\vec{\tau}_{\sigma\sigma'}}{2} f_{\sigma'}, \quad (19)$$

where  $\tau^{x,y,z}$  are the Pauli matrices. To stay within the Hilbert space for the spin, we assign an energy  $\lambda$  to the  $f$ -electron level and calculate any correlation function ( $\mathcal{D}$ ) involving the spin from the corresponding correlation function in the  $f$ -electron representation ( $\tilde{\mathcal{D}}$ ) using

$$\mathcal{D} = \lim_{\lambda \rightarrow \infty} \frac{1}{2} e^{\beta\lambda} \tilde{\mathcal{D}}. \quad (20)$$

Here the prefactor  $\frac{1}{2} e^{\beta\lambda}$  is introduced to compensate the Boltzmann weighting factor for the singly occupied subspace in the pseudo-fermion basis. Wick's theorem applies to  $\tilde{\mathcal{D}}$  since it involves only canonical fermion operators.

Fig. 2 shows the diagrammatic representation of the bare propagators:

$$G_f^b(i\omega_n) = \frac{1}{i\omega_n - \lambda} \quad (21)$$

for the  $f$ -electron,

$$G^b(p, i\omega_n) = \frac{1}{i\omega_n - E_p} \quad (22)$$

for the conduction electrons, and

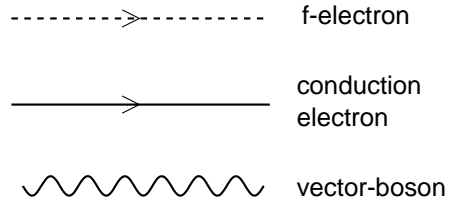


FIG. 2. Bare propagators of the impurity problem defined by the Hamiltonian (7), with the spin of the local moment represented in terms of (pseudo-) $f$ -electrons.

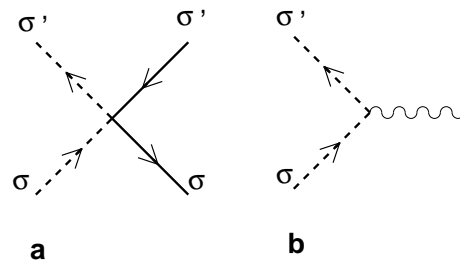


FIG. 3. (a) Kondo coupling between the spin of an  $f$ -electron and the spin of a conduction electron; (b) coupling between the spin of an  $f$ -electron and the vector-boson field.

$$G_{\phi}^b(p, i\nu_m) = \frac{2w_p}{(i\nu_m)^2 - w_p^2} \quad (23)$$

for the vector bosons.  $G_{\phi}^b(p, i\nu_m)$  is the Fourier transform of  $G_{\phi}^b(p, \tau) \equiv -\langle T_{\tau}(\vec{\phi}_p + \vec{\phi}_{-p}^{\dagger})(\tau) \cdot (\vec{\phi}_p + \vec{\phi}_{-p}^{\dagger})(0) \rangle / 3$ .

In the pseudo-fermion representation, the Hamiltonian terms describing the Kondo interaction and the local moment-vector boson interaction take the forms

$$H_J = \frac{J_K}{4} \sum_{\sigma\sigma'} \sigma\sigma' f_{\sigma}^{\dagger} f_{\sigma} c_{\sigma'}^{\dagger} c_{\sigma'} + \frac{J_K}{2} (f_{\uparrow}^{\dagger} f_{\downarrow} c_{\downarrow}^{\dagger} c_{\uparrow} + \text{H.c.}), \quad (24)$$

$$H_g = \frac{g}{2} \sum_{\sigma} \sigma f_{\sigma}^{\dagger} f_{\sigma} \phi^z + \frac{g}{\sqrt{2}} (f_{\uparrow}^{\dagger} f_{\downarrow} \phi^{-} + \text{H.c.}),$$

where  $\sigma, \sigma' = \pm 1$ ,  $\vec{\phi} = \sum_p (\vec{\phi}_p + \vec{\phi}_{-p}^{\dagger})$ , and  $\phi^{\pm} = (\phi^x \pm \phi^y) / \sqrt{2}$ .  $H_J$  and  $H_g$  are shown graphically in Fig. 3.

### A. RG equations

We first determine the bare scaling dimensions of the couplings  $J_K$  and  $g$ .  $\mathbf{S}(\tau)$  is dimensionless because when  $J_K = g = 0$ ,  $\langle \mathbf{S}(\tau) \cdot \mathbf{S}(0) \rangle_0$  is a constant.  $\vec{\phi}(\tau)$  has the scaling dimension of  $\tau^{-(1+\gamma)/2}$ , and  $\mathbf{s}_c(\tau)$  that of  $\tau^{-1}$ . Therefore,  $J_K$  is marginal, while  $g$  has scaling dimension  $(1-\gamma)/2$ , i.e.,  $g$  is marginal for  $\gamma = 1$  and relevant for  $\gamma < 1$ .

We now calculate the  $\beta$  function to cubic order in the coupling constants. To do so, we first calculate the perturbative contributions to the  $f$ -electron self-energy,

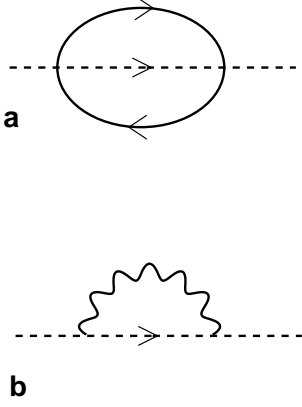


FIG. 4. Diagrams for the  $f$ -electron self-energy.

and the perturbative corrections to the vertices shown in Fig. 3. (The self-energies of the fermionic and bosonic baths are of order  $1/N_{\text{site}}$  and vanish in the thermodynamic limit for the baths or, equivalently, when the bath spectra are continuous.) Details of the calculation are given in Appendix A.

Consider first the  $f$ -electron self-energy. The relevant diagrams for the perturbative corrections are given in Fig. 4. The result is:

$$\Sigma_f(\omega + \lambda) = - \left[ \frac{3}{8}(N_0 J_K)^2 + \frac{3}{4}(K_0 g)^2 \right] \omega \ln \frac{W}{\omega}, \quad (25)$$

where  $W$  is a running cutoff energy. Introducing  $\mathcal{G}_f$  through

$$G_f(\omega + \lambda) = \mathcal{G}_f^b(\omega + \lambda) \mathcal{G}_f(\omega), \quad (26)$$

we have

$$\mathcal{G}_f(\omega) = 1 - \left[ \frac{3}{8}(N_0 J_K)^2 + \frac{3}{4}(K_0 g)^2 \right] \ln \frac{W}{\omega}. \quad (27)$$

Next consider the corrections to the Kondo coupling  $J_K$ . Due to spin-rotational invariance it suffices to examine just the spin-flip processes, say. Also, we set the energy of the external  $f$ -electrons to  $\omega + \lambda$  and that of the external conduction electrons to  $\mu$ . The diagrams that lead to singular corrections to the full vertex  $\Gamma_J(\omega)$  are given in Fig. 5. We write the full vertex as

$$\Gamma_J(\omega) = J_K \gamma_J(\omega), \quad (28)$$

and find that

$$\gamma_J(\omega) = 1 + \left[ N_0 J_K - \frac{1}{8}(N_0 J_K)^2 - \frac{1}{4}(K_0 g)^2 \right] \ln \frac{W}{\omega}. \quad (29)$$

Finally, consider the corrections to the coupling constant  $g$ . The diagrams contributing singular corrections to the corresponding full vertex  $\Gamma_g$  are given in Fig. 6. Writing

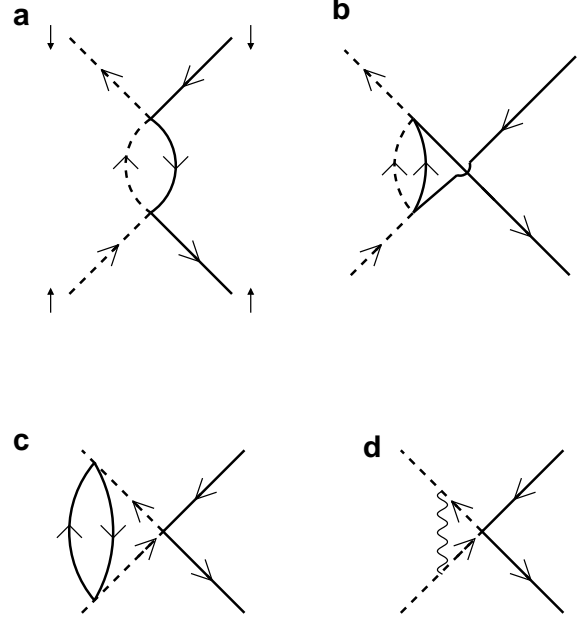


FIG. 5. Perturbative corrections to the Kondo coupling vertex.

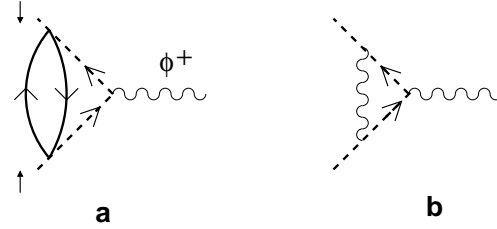


FIG. 6. Perturbative corrections to the vertex describing the coupling of the local moment to the vector bosons.

$$\Gamma_g(\omega) = g \gamma_g(\omega), \quad (30)$$

we have

$$\gamma_g(\omega) = 1 - \left[ \frac{1}{8}(N_0 J_K)^2 + \frac{1}{4}(K_0 g)^2 \right] \ln \frac{W}{\omega}. \quad (31)$$

We are now in a position to construct the RG equations. Lowering the cutoff energy from  $W$  to  $W'$  produces the coupling-constant and wave-function renormalizations

$$\begin{aligned} \mathcal{G}_f(\omega, W', J'_K, g') &= z_f \mathcal{G}_f(\omega, W, J_K, g), \\ \gamma_J(\omega, W', J'_K, g') &= z_J^{-1} \gamma_J(\omega, W, J_K, g), \\ \gamma_g(\omega, W', J'_K, g') &= z_g^{-1} \gamma_g(\omega, W, J_K, g), \end{aligned} \quad (32)$$

where

$$J'_K = z_f^{-1} z_J J_K, \quad g' = z_f^{-1} z_g g. \quad (33)$$

This leads to the RG equations

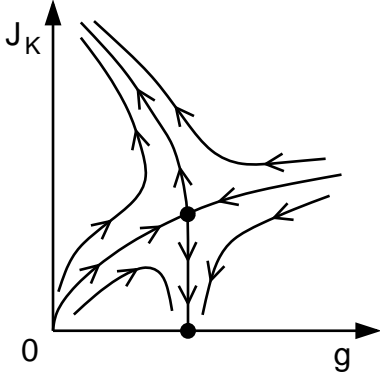


FIG. 7. Schematic RG flow of the Bose-Fermi Kondo model. Note the unstable fixed point at finite  $J_K$  and  $g$ .

$$\begin{aligned} \frac{dJ_K}{dl} &= J_K \left[ N_0 J_K - \frac{1}{2} N_0^2 J_K^2 - K_0^2 g^2 \right], \\ \frac{dg}{dl} &= g \left[ \frac{1-\gamma}{2} - \frac{1}{2} N_0^2 J_K^2 - K_0^2 g^2 \right], \end{aligned} \quad (34)$$

where  $l = \ln(W/W')$ .

To linear order in  $1-\gamma$ , the  $\beta$  functions given in Eq. (34) yield an unstable fixed point located in the  $J_K$ - $g$  plane at

$$(K_0 g^*)^2 = N_0 J_K^* = (1-\gamma)/2. \quad (35)$$

A separatrix passes through this critical point and through the origin,  $J_K = g = 0$ : to its left (right) in the  $J_K$ - $g$  plane the RG flow of  $J_K$  is towards infinity (zero) (see Fig. 7). For small  $J_K$  and  $g$ , the position of the separatrix, expressed in the form  $g_c(J_K)$ , can be determined by iterating the RG flow. This calculation, the details of which appear in Appendix B, gives

$$(K_0 g_c)^2 = 2(1-\gamma) \exp\left(-\frac{1-\gamma}{N_0 J_K}\right). \quad (36)$$

## B. Correlation functions at the critical point

Consider first the local spin autocorrelation function

$$\chi_{\text{loc}}(\tau) \equiv \langle T_\tau S^x(\tau) S^x(0) \rangle = \lim_{\lambda \rightarrow \infty} \frac{1}{2} e^{\beta\lambda} \tilde{\chi}(\tau), \quad (37)$$

where

$$\tilde{\chi}(\tau) \equiv \frac{1}{2} \langle T_\tau f_\downarrow^\dagger(\tau) f_\uparrow(\tau) f_\uparrow^\dagger(0) f_\downarrow(0) \rangle, \quad (38)$$

which can be calculated using diagrammatic techniques. The correlation functions along the entire separatrix specified by Eq. (36) are asymptotically the same as their counterparts at the fixed point described by Eq. (35).

As usual, given that  $1-\gamma$  is treated as an expansion parameter, the correlation functions at the critical point can be calculated via perturbative expansion in the couplings  $J_K$  and  $g$ , at the end replacing these couplings by their fixed-point values,  $J_K^*$  and  $g^*$ , respectively. The low-order diagrams are shown in Figs. 8(a)–(g).

Because  $J_K^*$  is of order  $1-\gamma$ , the corrections to  $\chi_{\text{loc}}$  from the Kondo coupling  $J_K$  [Figs. 8(e), 8(f), and 8(g)] are of higher-than-linear order in  $1-\gamma$ . The calculation of the remaining contributions is given in detail in Appendix C. Diagram 8(a) contributes to zeroth order in  $1-\gamma$ :

$$\chi_{\text{loc}}^{(a)}(\tau) = 1/4. \quad (39)$$

Three diagrams contribute to first order in  $1-\gamma$ . The singular correction from diagram 8(b) is

$$\chi_{\text{loc}}^{(b)}(\tau) = -\frac{1}{8} (K_0 g^*)^2 \ln \frac{\sin(\pi\tau/\beta)}{\pi/\Lambda\beta}. \quad (40)$$

(Here we consider  $0 < \tau < \beta$ .) The singular contributions from diagrams 8(c) and 8(d) sum to

$$\chi_{\text{loc}}^{(cd)}(\tau) = -\frac{3}{8} (K_0 g^*)^2 \ln \frac{\sin(\pi\tau/\beta)}{\pi/\Lambda\beta}. \quad (41)$$

Collecting all these contributions, noting that  $(K_0 g^*)^2 = (1-\gamma)/2$ , and following the procedure of the standard  $\epsilon$ -expansion,<sup>43</sup> we end up with the following form for the local spin correlation function at the critical point:

$$\chi_{\text{loc}}(\tau) = \frac{1}{4} \left( \frac{\pi/\Lambda\beta}{\sin(\pi\tau/\beta)} \right)^{1-\gamma}. \quad (42)$$

In the zero-temperature limit, this gives, for  $0 < \gamma < 1$ ,

$$\chi_{\text{loc}}(\omega) = \frac{1}{2\Lambda^{1-\gamma}} \Gamma(\gamma) \sin \frac{\pi(1-\gamma)}{2} (-i\omega)^{-\gamma}, \quad (43)$$

where  $\Gamma$  is the gamma function, and for  $\gamma = 0$ ,

$$\chi_{\text{loc}}(\omega) = \frac{1}{2\Lambda} \ln \frac{\Lambda}{-i\omega}. \quad (44)$$

Now we turn to the conduction-electron Green's function. The leading nonvanishing contribution to the conduction-electron self-energy is given in Fig. 9. Since  $J_K^*$  is of order  $1-\gamma$ , we conclude that

$$\Sigma = O((1-\gamma)^2), \quad (45)$$

i.e., the conduction-electron Green's function is unrenormalized to linear order in  $1-\gamma$ . Note that this stands in marked contrast to the strong-coupling Kondo phase, where  $\Sigma$  has a pole.<sup>44</sup>

To summarize, for a fixed  $J_K$ , the impurity model displays a QCP at a critical coupling,  $g_c(J_K)$  specified by Eq. (36). The static impurity spin susceptibility diverges as  $g \rightarrow g_c^-$ , as illustrated in Fig. 10(a). At the QCP,

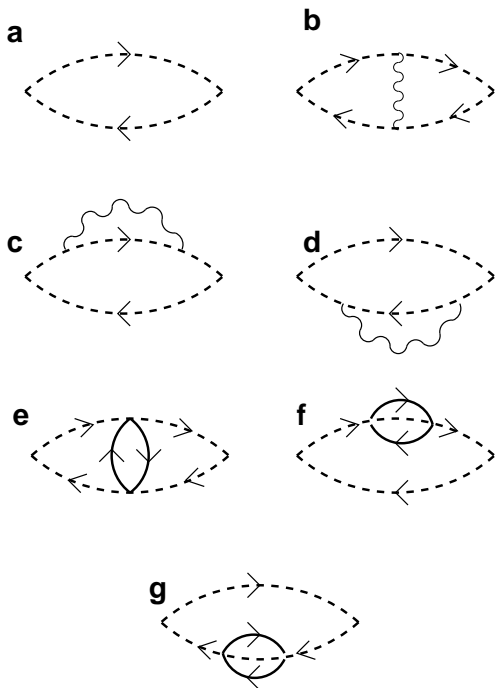


FIG. 8. Perturbation series for  $\tilde{\chi}_{\text{loc}}$ , defined in Eq. (38), showing terms entering at zeroth (a), first (b)–(d), and higher (e)–(g) order in  $1 - \gamma$ .

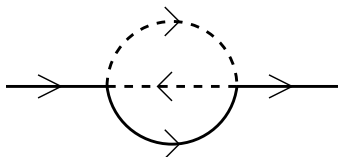


FIG. 9. Leading nonvanishing contribution to the conduction-electron self-energy.

the dynamical susceptibility is given by Eq. (43). Associated with this critical point is the vanishing of a local energy scale  $E_{\text{loc}}^*$ , reflecting a critical slowing down. This is shown schematically in Fig. 10(b). For  $g < g_c$ ,  $E_{\text{loc}}^*$  is finite and serves as an effective Fermi energy scale.

Subsequent to the work reported here, the RG analysis of the Bose-Fermi Kondo model has been extended<sup>45,46</sup> to higher orders in  $1 - \gamma$ . An unstable fixed point has been identified not only in the spin-isotropic model considered above, but also in the presence of anisotropy. In both cases, the exponent of the local spin correlation function at the critical point turns out to be  $1 - \gamma$  to all orders in  $1 - \gamma$ , in agreement with Eq. (42).

We note that power-law behavior of local spin-correlation functions has also been discussed in impurity models that arise in the context of quantum spin-glasses.<sup>47,40,48,49</sup> There, it is associated with a *stable* fixed point (i.e., a phase) of the impurity model. By contrast, what we have discussed above is an *unstable* fixed point

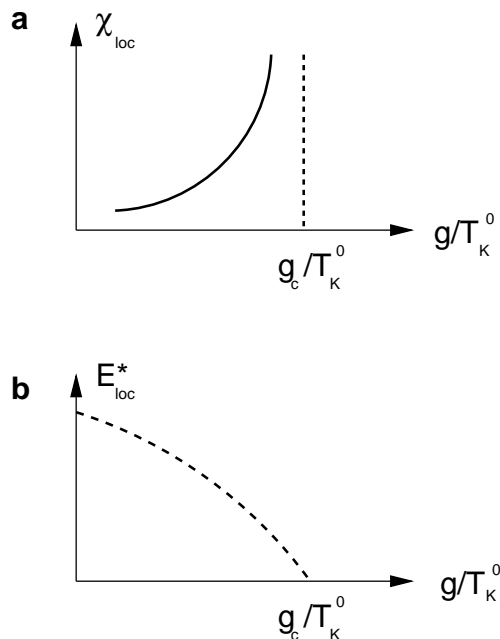


FIG. 10. (a) Static local spin susceptibility as a function of  $g/T_K^0$ . For  $g < g_c$ , the susceptibility is finite and the local moment is completely quenched. The divergence of the susceptibility at  $g = g_c$  signals that the dynamics of the local moment have become critical. (b) The local energy scale  $E_{\text{loc}}^*$  as a function of  $g/T_K^0$ .  $E_{\text{loc}}^*$  vanishes at  $g_c$ , reflecting a critical slowing down.

(a critical point).

#### IV. SELF-CONSISTENT SOLUTION

We must now address two key questions:

- Can the critical point associated with the local problem coincide with the magnetic ordering transition?
- What can cause the fluctuating magnetic field to have a sub-ohmic spectrum ( $\gamma < 1$ )?

The answer to both questions lies in the self-consistency requirement. The determining factor turns out to be the form of the RKKY density of states defined in Eq. (5). The significance of  $\rho_I(\epsilon)$  is that it characterizes the way the RKKY interaction enters the self-consistency condition. Indeed, combining Eq. (5) with Eq. (3), we can rewrite the first equation in the self-consistency condition (13) as

$$\chi_{\text{loc}}(\omega) = \int d\epsilon \frac{\rho_I(\epsilon)}{M(\omega) + \epsilon}. \quad (46)$$

We consider two types of RKKY density of states  $\rho_I(\epsilon)$ : The first type increases from the lower band edge (at  $\epsilon = I_{\mathbf{Q}}$ ) with a jump, as shown in Fig. 11(a). The second



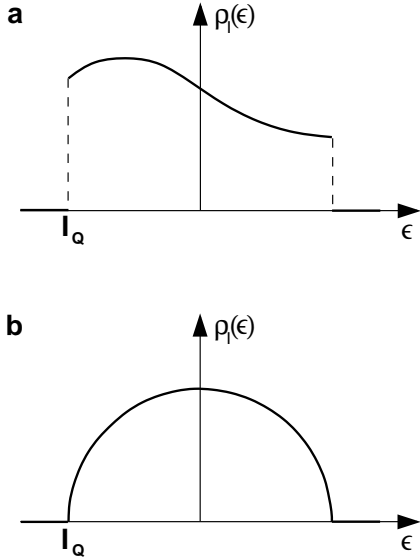


FIG. 11. (a) An RKKY density of states with a jump at the lower edge,  $\epsilon = I_{\mathbf{Q}}$ , characteristic of two-dimensional magnetic fluctuations; (b) An RKKY density of states with a square-root onset at the lower edge, characteristic of three-dimensional magnetic fluctuations.

type increases from the lower band edge in a square-root fashion, i.e., as  $\sqrt{\epsilon - I_{\mathbf{Q}}}$ . This is illustrated in Fig. 11(b).

The jump and square-root onset at the lower edge are characteristic of magnetic fluctuations in two dimensions and three dimensions, respectively. This can be seen, for instance, by comparing the form of the RKKY density of states for nearest-neighbor real-space coupling on a (two-dimensional) square lattice, where  $I_{\mathbf{Q}} = I(\cos q_x a + \cos q_y a)$ , and a (three-dimensional) cubic lattice, where  $I_{\mathbf{Q}} = I(\cos q_x a + \cos q_y a + \cos q_z a)$ .

In the remainder of this section, we describe the quantum critical behavior for the two types of RKKY density of states. The quantum phase transition takes place as the ratio of the RKKY interaction to the Kondo coupling,

$$\delta \equiv \frac{|I_{\mathbf{Q}}|}{T_K^0}, \quad (47)$$

is tuned through some critical value  $\delta_c$ , which labels the QCP. We expect  $\delta_c$ , the ratio of energy scales characterizing the competing interactions that give rise to the transition, to be of order unity.

The QCP is signaled by the divergence of the static spin susceptibility at the peak wavevector  $\mathbf{Q}$ . The peak susceptibility is related to the spin self-energy  $M(\omega)$  via Eq. (3):

$$\chi(\mathbf{Q}, \omega) = \frac{1}{M(\omega) + I_{\mathbf{Q}}}. \quad (48)$$

This implies that at the QCP,

$$M(\omega \rightarrow 0) = -I_{\mathbf{Q}}. \quad (49)$$

## A. Self-consistent solution in two dimensions

With a jump in the RKKY density of states, the self-consistency equation Eq. (46) can be written as

$$\chi_{\text{loc}}(\omega) = \int_{I_{\mathbf{Q}}}^{I_{\mathbf{Q}}+\Lambda_0} d\epsilon \frac{\rho_I(\epsilon)}{M(\omega) + \epsilon} + \int_{I_{\mathbf{Q}}+\Lambda_0} d\epsilon \frac{\rho_I(\epsilon)}{M(\omega) + \epsilon}, \quad (50)$$

where  $\Lambda_0$  is defined such that, for  $\epsilon \in (I_{\mathbf{Q}}, I_{\mathbf{Q}}+\Lambda_0)$ ,  $\rho_I(\epsilon)$  is approximately equal to its value at the lower edge,  $\rho_I(I_{\mathbf{Q}})$ . For instance, if  $\rho_I(\epsilon)$  is flat, then  $\Lambda_0$  is equal to the separation between the upper and lower edge of the flat  $\rho_I(\epsilon)$ . For a generic  $\rho_I(\epsilon)$ ,  $\Lambda_0$  is of the order of the RKKY interaction as parametrized by, say,  $|I_{\mathbf{Q}}|$ . Given Eq. (49), the first term in Eq. (50) is singular; the second term, on the other hand, is nonsingular and can be neglected. The self-consistency equation then becomes

$$\chi_{\text{loc}}(\omega) = \rho_I(I_{\mathbf{Q}}) \ln \frac{\Lambda_0}{M(\omega) + I_{\mathbf{Q}}}. \quad (51)$$

Eq. (51), when combined with Eqs. (48) and (49), leads to the conclusion that the local susceptibility  $\chi_{\text{loc}}(\omega \rightarrow 0)$  becomes singular at the same value of  $\delta$  where the peak susceptibility  $\chi(\mathbf{Q}, \omega \rightarrow 0)$  becomes singular. As usual, the singularity in  $\chi(\mathbf{Q}, \omega)$  signals the emergence of a critical mode associated with the long-wavelength fluctuations of the order parameter. However, from Section III B [see the discussion concerning Fig. 10(a)], we know that the divergence of  $\chi_{\text{loc}}(\omega)$  signifies the emergence of critical but spatially local modes; thus, the fluctuations of the local moments are also critical. The corresponding energy scale  $E_{\text{loc}}^*$  vanishes [Fig. 10(b)].

This reasoning leads to one of our key conclusions concerning the quantum critical behavior of the Kondo lattice in two dimensions: as we increase the parameter  $\delta$ , spatially local critical modes emerge simultaneously with the usual long-wavelength critical modes.

We now determine the detailed dynamics at the QCP, beginning with the conduction-electron self-energy. Since the effective impurity model is at its own critical point, our result of the previous section [Eq. (45)] implies that  $\Sigma$  vanishes to linear order in  $1 - \gamma$ . This shows that the fermion-bath density of states, assumed to be  $N_0$  in Eq. (14), is indeed a nonzero constant and is, in fact, equal to the bare conduction-electron density of states [see Eq. (2)] at the chemical potential:

$$N_0 = \rho_0(\mu). \quad (52)$$

Let us turn to the dynamical spin susceptibility. Combining Eq. (51) with Eq. (11) yields

$$\begin{aligned} \chi_0^{-1}(\omega) + \frac{1}{\chi_{\text{loc}}(\omega)} &= M(\omega) \\ &= -I_{\mathbf{Q}} + \Lambda_0 \exp \left[ -\frac{\chi_{\text{loc}}(\omega)}{\rho_I(I_{\mathbf{Q}})} \right]. \end{aligned} \quad (53)$$

Inserting Eqs. (16), (36), and (43) into Eq. (53), and demanding a power-law form for the frequency-dependent

part of the spin self-energy  $M(\omega)$ , we reach the following self-consistent solution for the parameters introduced in Eqs. (15)–(17):

$$\gamma = 0^+, \quad \Lambda = C/\pi = \frac{2}{\pi} T_K^0, \quad (54)$$

where  $T_K^0$  is defined in Eq. (18). The specific form for the spectral function of the vector-bosonic Weiss field is

$$\text{Im}\chi_0^{-1}(\omega + i0^+) = \pi\Lambda \left( \ln \frac{\Lambda}{|\omega|} \right)^{-2} \text{sgn } \omega, \quad (55)$$

while the local susceptibility is

$$\chi_{\text{loc}}(\omega + i0^+) = \frac{1}{2\Lambda} \ln \frac{\Lambda}{-i\omega}. \quad (56)$$

The spin self-energy is given in terms of  $\chi_{\text{loc}}$  through the second equality of Eq. (53). The result is

$$M(\omega) = -I_{\mathbf{Q}} + \Lambda_0(-i\omega/\Lambda)^\alpha, \quad (57)$$

where the exponent is

$$\alpha = \frac{1}{2\Lambda\rho_I(I_{\mathbf{Q}})}. \quad (58)$$

The parameter  $\Lambda$  is determined by the Kondo coupling, as shown in Eq. (54). The parameter  $\rho_I(I_{\mathbf{Q}})$ , introduced earlier, is the RKKY density of states at the lower edge [Fig. 11(a)].

We note that the local susceptibility at the critical point, given in Eq. (56), is universal. The exponent  $\alpha$  for the spin self-energy, on the other hand, depends on the product  $\Lambda\rho_I(I_{\mathbf{Q}})$ . Since the QCP is reached through competition between the RKKY and Kondo interactions, we expect that this product is close to unity, resulting in an  $\alpha$  that is not too far from  $\frac{1}{2}$ . The precise value of this product, however, is nonuniversal: it depends on which point of the phase boundary in the two-dimensional ( $|I_{\mathbf{Q}}|$ - $T_K^0$ ) parameter space is crossed as the system is tuned through the quantum phase transition (see Fig. 12).

The phase boundary can, in principle, be located by inserting Eq. (49) into Eq. (53). Recognizing that  $1/\chi_{\text{loc}}(\omega \rightarrow 0) = 0$ , one obtains the condition

$$\chi_0^{-1}(\omega \rightarrow 0) = -I_{\mathbf{Q}}. \quad (59)$$

In this paper we have carried out an asymptotic low-energy analysis of our dynamical equations. By contrast,  $\chi_0^{-1}(\omega \rightarrow 0)$  depends (through the Kramers-Kronig relation) on the solution at all energies. Therefore, the determination of the phase boundary and, hence, the value of the exponent  $\alpha$ , requires a complete (numerical) treatment of the problem. Recently, such a treatment has been carried out for a Kondo lattice model with Ising RKKY couplings.<sup>50,51</sup> A locally critical quantum phase transition was identified,<sup>50</sup> with a near-universal exponent  $\alpha = 0.72 \pm 0.01$ . Extension of such numerical work

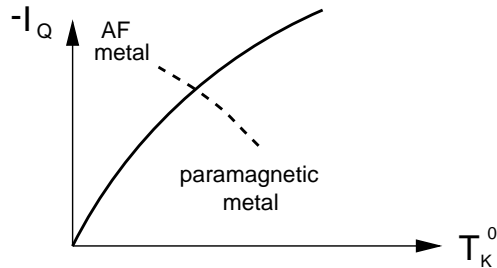


FIG. 12. Phase diagram of the Kondo lattice in the  $|I_{\mathbf{Q}}|$ - $T_K^0$  parameter space. The solid line is the phase boundary. The dashed line shows the tuning trajectory through the quantum phase transition for a given system.

to the isotropic case considered in the present paper remains an important problem for the future.

Fig. 12 also illustrates the important point that, in a given system, there is only one parameter that must be tuned to drive the system through criticality. The dashed line represents such a tuning trajectory.

Two additional remarks are in order. First, the self-consistent Weiss field  $\chi_0^{-1}$ , given in Eq. (55), has a logarithmic dependence. In (imaginary) time, this corresponds to an interaction with an algebraic component,  $1/\tau$ , multiplied by a logarithmic correction. On the other hand, the self-consistent solution for the spin-spin correlation function at the critical point, given by Eq. (56), corresponds to  $1/\tau$ , with no logarithmic correction. Within the  $(1-\gamma)$ -expansion carried out in Section III, the logarithmic corrections to the range of the interaction do not affect the critical exponent for  $\chi_{\text{loc}}$ , which remains algebraic without any logarithmic corrections. We believe that this remains true beyond the  $(1-\gamma)$ -expansion, since the spin-spin correlation functions at a critical point are in general algebraic and admit no logarithmic corrections. For the particular form of the self-consistent Weiss-field  $\chi_0^{-1}$  used here, we can demonstrate this point explicitly in a spherical model with a long-range interaction specified by  $\chi_0^{-1}$  (see Appendix D).

Second, the self-consistency equation (53) dictates that, at the critical point, the imaginary part of the spin-self-energy  $\text{Im}M(\omega)$  is sub-leading compared to both  $\text{Im}\chi_0(\omega)$  and  $\text{Im}\chi_{\text{loc}}(\omega)$ . In principle, we should allow a sub-leading term in  $\chi_0(\omega)$ , and determine both the leading and the sub-leading terms for the critical  $\chi_{\text{loc}}(\omega)$ . Calculating the sub-leading terms of  $\chi_{\text{loc}}(\omega)$  is, however, beyond the scope of the  $(1-\gamma)$ -expansion. What we have done, instead, is to take advantage of the freedom to choose the Weiss field such that the self-consistency equation is satisfied; Eq. (53), then, allows us to determine  $M$  from the leading term of  $\chi_{\text{loc}}(\omega)$ .

## B. Self-consistent solution in three dimensions

If the RKKY density of states increases at the lower band edge in a square-root fashion,

$$\lim_{\epsilon \rightarrow I_{\mathbf{Q}}^+} \rho_I(\epsilon) \propto \sqrt{\epsilon - I_{\mathbf{Q}}}, \quad (60)$$

the self-consistency equation (46) can again be written as in Eq. (50), the difference being that  $\Lambda_0$  is now defined such that the square-root form applies for  $\epsilon \in (I_{\mathbf{Q}}, I_{\mathbf{Q}} + \Lambda_0)$ . Again, for a generic  $\rho_I(\epsilon)$ ,  $\Lambda_0$  is of the order of the RKKY interaction  $|I_{\mathbf{Q}}|$ .

The second term on the right-hand side of Eq. (50) is finite, just as in two dimensions. In three dimensions, however, the first term—when combined with Eqs. (49) and (60)—also yields a finite value:

$$\int_{I_{\mathbf{Q}}}^{I_{\mathbf{Q}} + \Lambda_0} d\epsilon \frac{\rho_I(\epsilon)}{M(\omega) + \epsilon} \propto \sqrt{\Lambda_0}. \quad (61)$$

Thus, self-consistency dictates that in the three-dimensional case, the local susceptibility  $\chi_{\text{loc}}$  is finite at the QCP. Hence, from Section III B [see the discussion concerning Fig. 10(a)], we know that the dynamics of the local moment are not yet critical. Equivalently, the local energy scale  $E_{\text{loc}}^*$  is finite at the QCP.

We now proceed to extract the critical behavior. To be concrete, we work with a semi-circular form for the RKKY density of states:

$$\rho_I(\epsilon) = \frac{2}{\pi I^2} \sqrt{I^2 - \epsilon^2}, \quad (62)$$

for  $|\epsilon| \leq I$ . Solving the self-consistency equation (46) yields

$$M(\omega) = \left(\frac{I}{2}\right)^2 \chi_{\text{loc}}(\omega) + \frac{1}{\chi_{\text{loc}}(\omega)}, \quad (63)$$

which, when combined with Eq. (11), gives

$$\chi_0^{-1}(\omega) = (I/2)^2 \chi_{\text{loc}}(\omega). \quad (64)$$

The local physics is noncritical at the QCP, so the imaginary part of the spin self-energy should reflect the decay of spin fluctuations into particle-hole excitations and, hence, should be linear in frequency. We can quantify  $E_{\text{loc}}^*$  using the definition<sup>28</sup>

$$\text{Im}M^{-1}(\omega) = \omega/(E_{\text{loc}}^*)^2 \quad \text{for } |\omega| < E_{\text{loc}}^*. \quad (65)$$

Combined with Eq. (49), which now reads  $M(\omega \rightarrow 0) = I$ , this implies that

$$M(\omega) = I - i(I/E_{\text{loc}}^*)^2 \omega + O(\omega^2). \quad (66)$$

The precise value of  $E_{\text{loc}}^*$  can be determined using a technique that is applicable to the strong-coupling regime of the Bose-Fermi Kondo Hamiltonian, Eq. (7); one such method is slave-boson mean-field theory.<sup>44</sup>

Combining Eqs. (63) and (66) leads to the following form for the local susceptibility:

$$\chi_{\text{loc}}(\omega + i0^+) = \frac{2}{I} - \frac{2}{E_{\text{loc}}^*} \sqrt{\frac{2}{I}} \sqrt{-i\omega} - 2i\omega/(E_{\text{loc}}^*)^2 + O(\omega^{3/2}). \quad (67)$$

Using Eq. (64), the Weiss field is

$$\chi_0^{-1}(\omega + i0^+) = \frac{I}{2} - \frac{2}{E_{\text{loc}}^*} \left(\frac{I}{2}\right)^{3/2} \sqrt{-i\omega} - 2i(I/E_{\text{loc}}^*)^2 \omega + O(\omega^{3/2}). \quad (68)$$

We should stress that Eqs. (67) and (68) are compatible. In other words, for a given Bose-Fermi Kondo Hamiltonian [Eq. (7)] and given bath dispersions [Eqs. (14) and (15) with  $\gamma = 1/2$ ], the solution will yield an impurity dynamical spin susceptibility whose imaginary part is proportional to  $|\omega|^{1/2} \text{sgn} \omega$ . While the correlation functions on the strong-coupling side of the Bose-Fermi Kondo model are not accessible within the  $(1-\gamma)$ -expansion (and are in general difficult to determine except for certain large- $N$  limits), we note that the above is consistent with the bound set by Griffiths' theorem.<sup>52</sup> The correlation functions in the paramagnetic phase of the one-dimensional long-ranged spherical model provide additional support for this conclusion; see Appendix D.

## V. DYNAMICAL SPIN SUSCEPTIBILITY OF THE LOCALLY CRITICAL POINT AT FINITE TEMPERATURES

We now return to the locally critical point that occurs in the two-dimensional case. Inserting our  $T = 0$  solution for the spin self-energy, Eq. (57), into Eq. (3), we arrive at the following result for the momentum-dependent dynamical spin susceptibility at  $T = 0$ :

$$\chi(\mathbf{q}, \omega, T = 0) = \frac{1}{I_{\mathbf{q}} - I_{\mathbf{Q}} + \Lambda_0(-i\omega/\Lambda)^\alpha}, \quad (69)$$

where  $\Lambda_0$  is defined right after Eq. (50). We emphasize once again that the local susceptibility, given in Eq. (56), is universal. On the other hand, the exponent  $\alpha$  is not universal, as discussed after Eq. (58). It should also be noted that, for  $\mathbf{q} \sim \mathbf{0}$ , Eq. (69) is expected to be valid only if the total spin is not conserved; in heavy fermions, this is the case as a result of the strong spin-orbit couplings. In the conserved case, it would be important to keep track of the momentum-dependence of the spin self-energy for small  $\mathbf{q}$ .

At finite temperatures, the self-consistent solution still has  $\gamma = 0^+$ . From Eq. (42), we have

$$\chi_{\text{loc}}(\tau) = \frac{1}{4} \frac{\pi/\Lambda\beta}{\sin(\pi\tau/\beta)}, \quad (70)$$

yielding

$$\chi_{\text{loc}}(\omega + i0^+, T) = \frac{1}{2\Lambda} \left[ \ln \frac{\Lambda}{2\pi T} - \psi \left( \frac{1}{2} - i \frac{\omega}{2\pi T} \right) \right], \quad (71)$$

where  $\psi$  is the digamma function.

The corresponding spin self-energy can be found using the second equality of Eq. (53). The result is

$$M(\omega + i0^+, T) = -I_{\mathbf{Q}} + \Lambda_0 (2\pi/\Lambda)^{\alpha} T^{\alpha} \mathcal{M}(\omega/T), \quad (72)$$

where

$$\mathcal{M}(\omega/T) = \exp[\alpha\psi(1/2 - i\omega/2\pi T)]. \quad (73)$$

The momentum-dependent dynamical spin susceptibility at finite temperatures follows from inserting Eq. (72) into Eq. (3):

$$\chi(\mathbf{q}, \omega, T) = \frac{1}{I_{\mathbf{q}} - I_{\mathbf{Q}} + \Lambda_0 (2\pi/\Lambda)^{\alpha} T^{\alpha} \mathcal{M}(\omega/T)}. \quad (74)$$

## VI. GINZBURG-LANDAU THEORY

### A. Gaussian critical point and its instability

In the picture of the  $T = 0$  SDW transition, there is only one type of critical degrees of freedom, namely, the long-wavelength fluctuations of the magnetic order parameter. The Ginzburg-Landau (GL) action is an extension of the standard  $\phi^4$  theory for a classical phase transition to allow for order-parameter fluctuations that take place not only in space but also in (imaginary) time.<sup>20,21,26,53</sup> The temporal fluctuations can be thought of as adding  $z$  dimensions, where  $z$  is the dynamic exponent. In the antiferromagnetic case ( $\mathbf{Q}$  being nonzero),  $z = 2$  and the action takes the form

$$\begin{aligned} \mathcal{S}_{\text{SDW}} &= \mathcal{S}_{\text{lw}}[\mathbf{m}(\mathbf{q} \sim \mathbf{Q}, \omega)] \\ &= \int d\mathbf{q} \int d\omega [r + (\mathbf{q} - \mathbf{Q})^2 + |\omega|] [\mathbf{m}(\mathbf{q}, \omega)]^2 \\ &+ u \prod_{i=1}^4 \int d\mathbf{q}_i \int d\omega_i \delta\left(\sum_i \mathbf{q}_i\right) \delta\left(\sum_i \omega_i\right) [\mathbf{m}]^4 \\ &+ \dots \end{aligned} \quad (75)$$

The effective dimensionality is  $d_{\text{eff}} = d + z$ . For  $d = 2$  or  $d = 3$ ,  $d_{\text{eff}}$  equals or exceeds the upper critical dimension of 4, so the critical point is Gaussian. The  $T = 0$  dynamical spin susceptibility assumes the mean-field (RPA) form:

$$\chi^G(\mathbf{q}, \omega) \sim \frac{1}{(\mathbf{q} - \mathbf{Q})^2 - i\omega}, \quad (76)$$

where the linear-in-frequency dependence comes from Landau damping (decay into particle-hole pairs). All the nonlinear couplings are irrelevant, so the corresponding relaxation rate is superlinear, leading to a violation of

$\omega/T$  scaling.<sup>26,21,54,55</sup> (This is very different from QCPs in insulators in two dimensions,<sup>56,57</sup> where the dynamic exponent is usually  $z = 1$  and the corresponding  $\phi^4$ -theory is below its upper critical dimension.)

It should be noted that for two-dimensional magnetic fluctuations, the local (i.e.,  $\mathbf{q}$ -averaged) dynamical spin susceptibility associated with  $\chi^G(\mathbf{q}, \omega)$  is, in fact, singular:

$$\chi_{\text{loc}}^G(\omega) \equiv \int d\mathbf{q} \chi^G(\mathbf{q}, \omega) \sim \ln \frac{1}{-i\omega}. \quad (77)$$

Within the SDW description [Eq. (75)], the nonlinear terms couple only the long-wavelength modes, so this singular  $\chi_{\text{loc}}^G$  is inconsequential. However, when local degrees of freedom play a central role from the outset—as is the case for the local moments in heavy fermions—this singularity can cause important nonlinear effects in the dynamics of the local objects. The preceding sections amount to a microscopic analysis of these nonlinear effects.

### B. Ginzburg-Landau action for the locally critical point

We now address the important question of whether the locally critical point is internally consistent beyond the microscopic (EDMFT) approximations.

The defining feature of a locally critical point is the coexistence of local and long-wavelength critical modes. The long-wavelength modes, as usual, capture the divergence of the correlation length in space. They reflect the fact that there is a broken symmetry in the antiferromagnetic metal, and the order parameter corresponding to this broken symmetry vanishes continuously as the critical point is approached from the ordered side. The local critical modes are additional critical modes. They arise from a subtle “ordering” on the paramagnetic metal side, which also disappears continuously as the critical point is approached from the paramagnetic side. The “ordering” is associated with the formation of Kondo singlets, a process which yields Kondo resonances and makes the local moments part of the electron fluid. It is reflected in the formation of a “large” Fermi surface, which encloses a volume that counts both the number of conduction electrons and the number of local moments.<sup>44</sup> The strength of these Kondo resonances is captured by a quasiparticle residue  $Z$ , associated with the states on such a large Fermi surface. Unlike the SDW case, at the locally critical point  $Z$  goes to zero over the entire large Fermi surface.

The GL action, then, has to be the sum of three parts:

$$\mathcal{S}_{\text{LCP}} = \mathcal{S}_{\text{lw}}[\mathbf{m}(\mathbf{q} \sim \mathbf{Q}, \omega)] + \mathcal{S}_{\text{loc}} + \mathcal{S}_{\text{mix}}. \quad (78)$$

Here,  $\mathcal{S}_{\text{lw}}$  is the same as in Eq. (75),  $\mathcal{S}_{\text{loc}}$  describes the couplings among the local critical modes alone, and  $\mathcal{S}_{\text{mix}}$  takes into account the coupling between the local and spatially extended degrees of freedom.

The notion that local fluctuations are part of the quantum critical theory is at first sight surprising, especially viewed from what is known about classical (finite-temperature) phase transitions. The universality class of a classical critical point is entirely determined by statics.<sup>58</sup> (Real-time dynamics are considered only after the statics have determined the universality class.<sup>59</sup>) Static fluctuations can be energetically favorable only if they occur at long distances. The universality class of a QCP, by contrast, depends on statics and dynamics (quantum fluctuations) on an equal footing. The mixing of statics and dynamics opens the door for local fluctuations to have low energies, provided that their fluctuations in (imaginary) time are slow.

We are now in a position to address the robustness of the locally critical point. In the microscopic analysis, we assumed that the spin self-energy and the electron self-energy are independent of the wavevectors  $\mathbf{q}$  and  $\mathbf{k}$ . Allowing a  $\mathbf{k}$  dependence in the conduction-electron self-energy will not affect our analysis, since we are away from half-filling and the conduction-electron density of states is expected to remain finite. We now argue that allowing a  $\mathbf{q}$  dependence in the spin self-energy leaves the locally critical point intact, provided that  $\alpha < 1$  (as is the case observed in  $\text{CeCu}_{6-x}\text{Au}_x$  and  $\text{YbRh}_2\text{Si}_2$ ). Consider first the contribution to the spin self-energy from the nonlinear couplings within  $\mathcal{S}_{\text{lw}}$ . The effective dimension  $d_{\text{eff}} = d + z = 2 + 2/\alpha$  still exceeds 4, so all the nonlinear couplings within  $\mathcal{S}_{\text{lw}}$  must be irrelevant in the RG sense. The  $\mathbf{q}$  dependence of the spin self-energy will then be at most  $(\mathbf{q} - \mathbf{Q})^2$ . Consider next the contribution to the spin self-energy from  $\mathcal{S}_{\text{mix}}$ . Since the spin modes are coupled to the local modes, the corresponding contribution cannot have a singular  $\mathbf{q}$  dependence, either. As a result, the spatial anomalous dimension  $\eta$  takes the value  $\eta = 0$ , and the zero-temperature, zero-frequency spin susceptibility for  $\mathbf{q} \sim \mathbf{Q}$  goes as

$$\chi(\mathbf{q}) \sim \frac{1}{(\mathbf{q} - \mathbf{Q})^2}. \quad (79)$$

The corresponding local susceptibility remains singular. Therefore, the local criticality is robust.

We emphasize that the locally critical point is non-Gaussian because the appropriate field theory is *not* just the usual  $\phi^4$  theory, but instead has the form given in Eq. (78) above. Each of the three parts making up  $\mathcal{S}_{\text{LCP}}$  contains nonlinear couplings which flow under the RG transformation.  $\mathcal{S}_{\text{lw}}$  (the  $\phi^4$  theory) contains nonlinear couplings purely between long-wavelength modes. Since the effective dimensionality satisfies  $d_{\text{eff}} = d + z > 4$ , all these couplings are irrelevant, and they will contribute to the spin relaxation rate a term that is superlinear in  $T$ .<sup>21,26</sup> However,  $\mathcal{S}_{\text{loc}}$  and  $\mathcal{S}_{\text{mix}}$  contain nonlinear couplings involving the local modes. Some of these couplings are relevant, and will generate a linear-in- $T$  contribution to the spin relaxation rate. The total relaxation rate will be dominated by this second type of contribution, and will be linear in  $T$ , giving rise to  $\omega/T$  scaling in

the dynamical spin susceptibility. Our microscopic theory provides a specific prescription for determining this relaxation rate, as well as the universal scaling functions.

We close this subsection with a brief comment on the general validity of the EDMFT analysis of quantum critical behavior in metals. We have seen that, for the EDMFT results to be valid, it is crucial<sup>27</sup> that the critical point has a mean-field exponent for spatial fluctuations, i.e.,  $\eta = 0$ . (The temporal fluctuations are allowed to have an anomalous exponent.) This requires the nonlinear couplings among the long-wavelength modes to be irrelevant, a condition that is relatively easy to satisfy at a  $T = 0$  transition in a metallic system. The results presented above serve as a concrete example where the spatial fluctuations are Gaussian but the temporal fluctuations are non-Gaussian. For critical points where  $\eta \neq 0$ , by contrast, the EDMFT is not expected to describe the correct critical properties. For instance, at finite-temperature transitions (where  $\eta$  is in general nonzero), the EDMFT yields a first-order transition.<sup>60,61,51,62,63</sup> However, quantum critical dynamics—including those at finite temperatures—are controlled by the QCP at  $T = 0$ , and are correctly captured by EDMFT calculations.

## VII. COMPARISON WITH EXPERIMENTS

We now compare our conclusions with existing experiments in heavy-fermion metals, and also make several predictions that can be tested in the future.

### A. Inelastic neutron scattering, magnetization, and NMR relaxation rate

Our theoretical result for the dynamical spin susceptibility near a locally critical point [Eq. (74)] can be rewritten

$$\chi(\mathbf{q}, \omega, T) = \frac{1}{f(\mathbf{q}) + AT^\alpha \mathcal{M}(\omega/T)}, \quad (80)$$

where  $A = \Lambda_0(2\pi/\Lambda)^\alpha$ , and  $f(\mathbf{q}) = I_{\mathbf{q}} - I_{\mathbf{Q}}$  vanishes at the peak wavevector ( $\mathbf{q} = \mathbf{Q}$ ) but is finite at other wavevectors. Equation (80) implies that the dynamical spin susceptibility at the peak wavevector satisfies an  $\omega/T$  scaling:

$$\chi(\mathbf{Q}, \omega, T) = \frac{1}{AT^\alpha \mathcal{M}(\omega/T)}, \quad (81)$$

where the scaling function  $\mathcal{M}(\omega/T)$  is given in Eq. (73). Eq. (81) is consistent with the inelastic neutron scattering results<sup>16,17</sup> on  $\text{CeCu}_{6-x}\text{Au}_x$  at the critical concentration  $x_c \approx 0.1$ , where it is found that the exponent  $\alpha \approx 0.75$ . ( $\omega/T$  scaling was reported<sup>14</sup> earlier in  $\text{UCu}_{5-x}\text{Pd}_x$  for  $x = 1$  and 1.5. This system, however, seems to contain strong disorder, the effects of which remain a subject of debate.<sup>14,15,64,65</sup>) The scaling function

used to fit the experiments is  $(1 - i\omega/aT)^\alpha$ , which behaves very similarly to Eq. (73). The neutron scattering results<sup>16,17</sup> at generic wavevectors have also been fitted to the form of Eq. (80), with the same exponent  $\alpha \approx 0.75$ .

In our theory, the locally critical picture arises if the magnetic fluctuations are two-dimensional. Within experimental resolution,  $f(\mathbf{q})$  goes to zero along lines in the three-dimensional Brillouin zone, implying that the magnetic fluctuations in the quantum critical regime are two-dimensional in real space in the frequency and temperature ranges that have been studied to date.<sup>18,19,16</sup> It should be noted, however, that the magnetic ordering for  $x > x_c$  is three-dimensional. To properly address the finite- $T$  magnetic ordering transition, it will be necessary to incorporate the (small) RKKY coupling in the third dimension.<sup>66</sup> Whether dimensional crossover eventually takes place at lower temperatures in the quantum critical regime is a question that should be addressed in future experiments. We hope that our work will provide a stimulus for this kind of (challenging) experiment. It is also desirable that neutron scattering be carried out at a QCP where the magnetic fluctuations are genuinely three-dimensional. In this regard, we note that a violation of  $\omega/T$  scaling has been reported<sup>9</sup> in  $\text{Ce}_{1-x}\text{La}_x\text{Ru}_2\text{Si}_2$ .

It also follows from Eq. (80) that the static and uniform spin susceptibility,  $\chi \equiv M/H$ , has a modified Curie-Weiss form:

$$\chi(T) = \frac{1}{\Theta + BT^\alpha}, \quad (82)$$

where  $\Theta = I_{\mathbf{q}=0} - I_{\mathbf{Q}}$  and  $B \approx \Lambda_0 \Lambda^{-\alpha} (2\pi)^\alpha \exp[\alpha\psi(1/2)]$ . Eq. (82) fits well<sup>16,17</sup> the magnetization data in  $\text{CeCu}_{6-x}\text{Au}_x$ .

There are indications that the modified Curie-Weiss susceptibility describes several other heavy-fermion metals near a QCP.<sup>1</sup> One such material is  $\text{YbRh}_2\text{Si}_2$ ,<sup>67</sup> which exhibits thermodynamic and transport properties very similar to those of  $\text{CeCu}_{6-x}\text{Au}_x$ , and has a layered structure that suggests the possibility of (quasi)-two-dimensional magnetic fluctuations. These characteristics make  $\text{YbRh}_2\text{Si}_2$  a promising candidate for local criticality. However, inelastic neutron scattering has yet to be performed in this system.

The local susceptibility given in Eq. (71) leads to a non-Korringa NMR spin-lattice relaxation rate,

$$\frac{1}{T_1} \sim \text{constant}. \quad (83)$$

(We have assumed that the hyperfine constant is not strongly  $\mathbf{q}$ -dependent.) This prediction might be tested using NMR measurements on the Cu sites in  $\text{CeCu}_{6-x}\text{Au}_x$  or the Si sites in  $\text{YbRh}_2\text{Si}_2$ .

## B. Fermi surface properties, Hall coefficient and other transport properties

On the paramagnetic side of a magnetic ordering QCP, the coherence energy scale ( $E_{\text{loc}}^*$ ) is finite. This signals<sup>44</sup> the formation of heavy quasiparticles, whose Fermi surface is “large” in the sense that its volume counts both the conduction electrons and the local moments. In the case of an SDW transition,  $E_{\text{loc}}^*$  remains finite through the QCP, and the Fermi surface remains large on the antiferromagnetic side (except for the folding of the Fermi surface due to a broken translational symmetry). By contrast,  $E_{\text{loc}}^*$  vanishes at a locally critical point, and the Fermi surface is “small” on the antiferromagnetic side,<sup>68</sup> i.e., its volume and topology are such that the single-electron excitations come entirely from the conduction electrons. Thus, the topology of the Fermi surface differentiates the antiferromagnetic metal phase on the ordered side of the locally critical transition from its counterpart for an SDW transition. Experimental probes of the Fermi surface, such as de Haas-van Alphen measurements, both inside the antiferromagnetic metal phase and close to the QCP, may be used to distinguish between the two types of quantum phase transition.

As a consequence of the large change in the Fermi-surface volume across a locally critical point, the Hall coefficient at zero temperature is expected to undergo a large jump at the QCP. This provides another potential test of the locally critical picture. (A more general discussion of the behavior of the Hall coefficient can be found in Ref. 54; see also Ref. 69.)

Finally, we consider the longitudinal resistivity. At an antiferromagnetic SDW critical point, only certain hot spots of the Fermi surface are affected by the critical fluctuations. In the clean limit, then, the resistivity is expected to retain a Fermi-liquid  $T^2$  form.<sup>70,31</sup> At a locally critical point, on the other hand, the entire Fermi surface is affected and the resistivity will have a non-Fermi-liquid form.

The change of the Fermi-surface volume is also expected to be manifested in the behavior of the residual resistivity as a function of the tuning parameter. This is best studied by using pressure or a magnetic field as the tuning parameter. (By contrast, tuning by chemical doping would also induce a significant change in the amount of disorder.) We note that the residual resistivity does seem to show dramatic changes across the pressure-driven QCP in  $\text{CeCu}_5\text{Au}$  (Ref. 71) and the field-driven QCP in  $\text{YbRh}_2\text{Si}_2$  (Ref. 72).

## VIII. CONCLUSIONS AND OUTLOOK

In this paper, we have identified a new class of quantum critical point in Kondo lattice systems. We have carried out an EDMFT analysis of the Kondo lattice model and found that, when the magnetic fluctuations are two-dimensional, a locally critical point arises. Here, critical

local modes coexist with the long-wavelength fluctuations of the order parameter. We have also argued that the locally critical point is robust beyond our microscopic calculations.

Our results explain the salient features of the experiments in several heavy-fermion systems. In particular, we have made comparisons with the existing experiments in  $\text{CeCu}_{6-x}\text{Au}_x$  and  $\text{YbRh}_2\text{Si}_2$ . We have also made a number of predictions concerning the NMR relaxation rate, the Fermi-surface volume, and the Hall coefficient.

The crucial ingredient of local criticality is the presence of spatially local critical modes. This contrasts with the standard critical theory, in which the only low-energy modes are long-wavelength fluctuations of the order parameter. For heavy fermions, the emergence of such critical local fluctuations can ultimately be traced to the fact that, as a result of the microscopic Coulomb blockade, local moments are “pre-formed” at intermediate energies.<sup>73</sup> At an SDW transition, the local moments disappear at sufficiently low energies; their quenching by the conduction-electron spins leaves only electron-like excitations (Kondo resonances). At a locally critical point, on the other hand, vestiges of the local moments persist to asymptotically low energies. Such local-moment physics is neglected in the SDW treatment of magnetic quantum critical points.

For Mott-Hubbard systems, the microscopic Coulomb blockade is responsible for the formation of the Mott insulator. One is therefore led to speculate that low-energy local modes may well play a key role in metals near a Mott transition. This issue is becoming increasingly important due to the observations of (nearly) quantum critical behavior in transition-metal oxides,<sup>74</sup> as well as the apparent scaling behavior in high-temperature superconductors.<sup>3,4,75,76</sup>

## ACKNOWLEDGMENTS

We thank E. Fradkin and S. Sachdev for useful discussions concerning logarithmic corrections in the Bose-Fermi Kondo model. This work has been supported in part by NSF Grant No. DMR-0090071 and TCSUH. Q.S. would also like to acknowledge the support of Argonne National Laboratory, the University of Chicago, and the University of Illinois at Urbana-Champaign during his sabbatical leave, and the hospitality of the Aspen Center for Physics.

## APPENDIX A: DERIVATION OF THE RG EQUATIONS

In this appendix, we present the derivation of the RG equations (34), following a procedure outlined in Ref. 39.

Consider first the pseudo- $f$ -electron self-energy. There are two contributions, as specified by Fig. 4. The contribution (a) is given by

$$\Sigma^{(a)}(i\omega_f) = -\frac{3}{8} \frac{J_K^2}{\beta^2} \sum_{p,p'} \sum_{i\omega_1} \sum_{i\omega_2} G_f^b(i\omega_1) \times G^b(p, i\omega_2) G^b(p', i\omega_f + i\omega_2 - i\omega_1). \quad (\text{A1})$$

Here the factor of 3 comes from summation over the three spin components. Carrying through the summation over  $i\omega_1$  and  $i\omega_2$ , setting  $i\omega_f = \omega + \lambda$ , and using the fact that  $\lambda \rightarrow \infty$ , we have

$$\begin{aligned} \Sigma^{(a)}(\omega + \lambda) &= \frac{3}{8} J_K^2 \sum_{p,p'} \frac{f(\epsilon_p)[1 - f(\epsilon_{p'})]}{\omega + \epsilon_p - \epsilon_{p'}} \\ &= -\frac{3}{8} (N_0 J_K)^2 \left[ 2D \ln 2 + \omega \ln \frac{D}{\omega} + O(\omega) \right], \quad (\text{A2}) \end{aligned}$$

where  $D$  is the half-bandwidth, and the Fermi factor  $f(\epsilon) = (e^{\beta\epsilon} + 1)^{-1}$ . Note that in the second line we have set  $T = 0$ , since our purpose here is to construct the RG equations.

Similarly,

$$\Sigma^{(b)}(i\omega_f) = -\frac{3}{4} \frac{g^2}{\beta} \sum_p \sum_{i\omega_1} G_f^b(i\omega_1) G_\phi^b(p, i\omega - i\omega_1). \quad (\text{A3})$$

To linear order in  $1 - \gamma$ , we can set  $\gamma = 1$  in  $G_\phi^b$  and the corresponding spectral function is

$$\begin{aligned} A_\phi(\epsilon) &\equiv -\frac{1}{\pi} \text{Im} \sum_p G_\phi^b(p, \epsilon + i0^+) \\ &= K_0^2 \epsilon \quad \text{for } |\epsilon| < \Lambda. \quad (\text{A4}) \end{aligned}$$

We then have

$$\begin{aligned} \Sigma^{(b)}(\omega + \lambda) &= \frac{3}{4} g^2 \int d\epsilon A_\phi(\epsilon) \frac{1 + n_B(\epsilon)}{\omega - \epsilon} \\ &= -\frac{3}{4} (K_0 g)^2 \left[ \Lambda + \omega \ln \frac{\Lambda}{\omega} + O(\omega) \right], \quad (\text{A5}) \end{aligned}$$

where the Bose factor  $n_B(\epsilon) = (e^{\beta\epsilon} - 1)^{-1}$ . The constant parts can be absorbed in a shift of  $\lambda$ . The  $\omega \ln \omega$  parts are retained in Eq. (25), where we have replaced the cutoffs by the running cutoff  $W$ .

We now turn to the corrections to the Kondo coupling, as given in Fig. 5. We set the external frequencies of the conduction electrons to 0, and those for the pseudo- $f$ -electrons to  $i\omega_f$ . The contribution from Fig. 5(a) is

$$\begin{aligned} \Gamma_J^{(a)}(\omega + \lambda) &= -\frac{J_K^2}{2\beta} \sum_p \sum_{i\omega_1} G^b(p, i\omega_1) G_f^b(i\omega_f + i\omega_1)|_{i\omega_f = \omega + \lambda} \\ &= -\frac{1}{2} J_K^2 N_0 \int d\epsilon \frac{f(\epsilon)}{\omega + \epsilon} = \frac{1}{2} J_K^2 N_0 \ln \frac{D}{\omega}, \quad (\text{A6}) \end{aligned}$$

where, in the second equality (and at similar places in the equations to follow) we take  $\lambda \rightarrow \infty$ . The contribution from Fig. 5(b) is

$$\begin{aligned}\Gamma_J^{(b)}(\omega+\lambda) &= \frac{J_K^2}{2\beta} \sum_{i\omega_1} \sum_p G^b(p, i\omega_1) G_f^b(i\omega_f - i\omega_1)|_{i\omega_f=\omega+\lambda} \\ &= -\frac{1}{2} J_K^2 N_0 \int d\epsilon \frac{1-f(\epsilon)}{\omega-\epsilon} = \frac{1}{2} J_K^2 N_0 \ln \frac{D}{\omega}.\end{aligned}\quad (\text{A7})$$

The contribution from Fig. 5(c) is

$$\Gamma_J^{(c)}(i\omega_f) = -\frac{J_K^3}{8\beta} \sum_{i\omega_1} \chi_c(i\omega_f - i\omega_1) [G_f^b(i\omega_1)]^2, \quad (\text{A8})$$

where  $\chi_c(i\omega)$  is the bare local conduction-electron susceptibility, which has a spectral function

$$A_{\chi_c} \equiv \frac{1}{\pi} \chi_c''(\epsilon + i0^+) = N_0^2 \epsilon. \quad (\text{A9})$$

The result is

$$\begin{aligned}\Gamma_J^{(c)}(\omega + \lambda) &= -\frac{1}{8} J_K^3 \int d\epsilon A_{\chi_c}(\epsilon) \frac{1+n_B(\epsilon)}{(\omega-\epsilon)^2} \\ &= -\frac{1}{8} J_K^3 N_0^2 \ln \frac{D}{\omega}.\end{aligned}\quad (\text{A10})$$

The contribution from Fig. 5(d) is

$$\Gamma_J^{(d)}(i\omega_f) = \frac{g^2 J_K}{4\beta} \sum_{i\omega_1} \sum_p G_\phi^b(p, i\omega_f - i\omega_1) [G_f^b(i\omega_1)]^2. \quad (\text{A11})$$

Using Eq. (A4), we have

$$\begin{aligned}\Gamma_J^{(d)}(\omega + \lambda) &= -\frac{1}{4} g^2 J_K \int d\epsilon A_\phi(\epsilon) \frac{1+n_B(\epsilon)}{(\omega-\epsilon)^2} \\ &= -\frac{1}{4} J_K (K_0 g)^2 \ln \frac{\Lambda}{\omega}.\end{aligned}\quad (\text{A12})$$

Finally, we consider the corrections to the coupling constant  $g$ . We set the external frequency for the  $\phi$  propagator to 0, and that for each pseudo- $f$ -electron propagator to  $i\omega_f$ . Then

$$\begin{aligned}\Gamma_g^{(a)}(\omega+\lambda) &= -\frac{gJ_K^2}{8\beta} \sum_{i\omega_1} \chi_c(i\omega_f - i\omega_1) [G_f^b(i\omega_1)]^2|_{i\omega_f=\omega+\lambda} \\ &= -\frac{1}{8} g (N_0 J_K)^2 \ln \frac{D}{\omega},\end{aligned}\quad (\text{A13})$$

and

$$\begin{aligned}\Gamma_g^{(b)}(\omega+\lambda) &= \frac{g^3}{4\beta} \sum_{i\omega_1} G_\phi^b(i\omega_f - i\omega_1) [G_f^b(i\omega_1)]^2|_{i\omega_f=\omega+\lambda} \\ &= -\frac{1}{4} g (K_0 g)^2 \ln \frac{D}{\omega}.\end{aligned}\quad (\text{A14})$$

Setting  $\omega = W'$  in Eq. (32) leads to

$$\begin{aligned}z_f &= 1 + \left[ \frac{3}{8} (N_0 J_K)^2 + \frac{3}{4} (K_0 g)^2 \right] \ln \frac{W}{W'} \\ z_J &= 1 + \left[ N_0 J_K - \frac{1}{8} (N_0 J_K)^2 - \frac{1}{4} (K_0 g)^2 \right] \ln \frac{W}{W'} \\ z_g &= 1 - \left[ \frac{1}{8} (N_0 J_K)^2 + \frac{1}{4} (K_0 g)^2 \right] \ln \frac{W}{W'}\end{aligned}\quad (\text{A15})$$

From Eq. (33), we have

$$\begin{aligned}J'_K &= J_K + J_K \left[ N_0 J_K - \frac{1}{2} (N_0 J_K)^2 - (K_0 g)^2 \right] \ln \frac{W}{W'} \\ g' &= g - g \left[ \frac{1}{2} (N_0 J_K)^2 + (K_0 g)^2 \right] \ln \frac{W}{W'}\end{aligned}\quad (\text{A16})$$

## APPENDIX B: DETERMINATION OF THE SEPARATRIX IN THE $J_K$ - $g$ PLANE FROM THE RG FLOW

Our starting point is the RG equations (34), which yield the RG flow shown in Fig. 7. We imagine approaching the separatrix from the local-moment side. The separatrix is identified when the initial parameters are such that  $N_0 J_K$  no longer flows to zero but instead is renormalized to its fixed-point value  $\sqrt{(1-\gamma)/2}$ .

Consider the separatrix near the origin. Provided that we work either on the local-moment side or on the separatrix itself,  $(N_0 J_K)^2$  is at most of the order of  $(1-\gamma)^2$  during the entire flow and can safely be ignored inside the brackets on the right-hand sides of both flow equations (34). (This is not the case on the Kondo side.) With this approximation, and the shorthand notation

$$a \equiv N_0 J_K, \quad b \equiv (K_0 g)^2, \quad (\text{B1})$$

the RG equations simplify to

$$\frac{da}{dl} = a(a-b), \quad (\text{B2})$$

$$\frac{db}{dl} = 2b \left[ \frac{1-\gamma}{2} - b \right]. \quad (\text{B3})$$

These equations have an unstable fixed point at

$$a^* = b^* = \frac{1-\gamma}{2}. \quad (\text{B4})$$

Solving Eq. (B3) yields

$$b = \frac{1-\gamma}{2} \left[ 1 + (c_0 - 1) e^{-(l-l_0)(1-\gamma)} \right]^{-1}. \quad (\text{B5})$$

Here,

$$c_0 \equiv \frac{1-\gamma}{2b_0}, \quad (\text{B6})$$

and  $b_0$  and  $l_0$  (as well as  $a_0$ ,  $z_0$ , and  $y_0$  used below) are the initial values of the corresponding parameters.

We can now proceed to solve Eq. (B2). Let us write

$$a = zy, \quad (\text{B7})$$

where the factor  $z$  is defined as satisfying

$$\frac{dz}{dl} = -bz. \quad (\text{B8})$$



When combined with Eq. (B5), Eq. (B8) can be easily solved to give

$$z = z_0 \left[ \frac{c_0 e^{-(l-l_0)(1-\gamma)}}{1 + (c_0 - 1)e^{-(l-l_0)(1-\gamma)}} \right]^{\frac{1}{2}}. \quad (\text{B9})$$

The other factor,  $y$ , satisfies the differential equation

$$\frac{dy}{dl} = zy^2, \quad (\text{B10})$$

which, when combined with Eq. (B9), leads to

$$y = y_0 \left[ 1 - \frac{a_0}{1-\gamma} \sqrt{c_0} A(l) \right]^{-1}, \quad (\text{B11})$$

where

$$A(l) \equiv \int_1^{e^{(l-l_0)(1-\gamma)}} \frac{d\lambda}{\lambda\sqrt{\lambda + c_0 - 1}}. \quad (\text{B12})$$

Using<sup>82</sup>

$$\int \frac{dx}{\sqrt{x}(a+bx)} = \frac{1}{i\sqrt{ab}} \ln \frac{a-bx+2i\sqrt{abx}}{a+bx} \quad \text{for } ab < 0, \quad (\text{B13})$$

and recognizing that, for parameters near the origin,  $c_0 \equiv (1-\gamma)/(2b_0) \ll 1$ , we obtain the following asymptotic form in the limit  $l-l_0 \gg 1/(1-\gamma)$ :

$$A(l \rightarrow \infty) \approx \frac{1}{\sqrt{c_0}} \ln(4c_0) - 2e^{-(l-l_0)(1-\gamma)/2}. \quad (\text{B14})$$

Combining Eqs. (B7), (B9), (B11), and (B14), we arrive at the asymptotic solution for  $a$ :

$$a(l \rightarrow \infty) \approx \frac{a_0 \sqrt{c_0} e^{-(l-l_0)(1-\gamma)/2}}{B + \frac{a_0 \sqrt{c_0}}{a^*} e^{-(l-l_0)(1-\gamma)/2}}, \quad (\text{B15})$$

where

$$B = 1 - \frac{a_0}{1-\gamma} \ln(4c_0). \quad (\text{B16})$$

It is now clear that when  $B$  is positive,  $a(l=\infty) = 0$ . In other words, the system falls in the local-moment regime. On the other hand,  $a(l=\infty) = a^*$  when  $B = 0$ , i.e., when

$$a_0 \ln(4c_0) = 1 - \gamma. \quad (\text{B17})$$

This condition specifies the separatrix. Written in terms of the original variables, through Eqs. (B1) and (B6), this becomes Eq. (36).

For completeness, we also write down the equation for the separatrix when the condition  $c_0 \gg 1$  is not satisfied. In this case,  $a(l)$  still has the asymptotic form specified by Eq. (B15), but Eq. (B16) is replaced by

$$B = 1 - \frac{a_0 \sqrt{c_0}}{(1-\gamma)\sqrt{c_0-1}} \ln \left[ 2c_0 - 1 + 2\sqrt{c_0(c_0-1)} \right], \quad (\text{B18})$$

and Eq. (B17) is modified accordingly. It is straightforward to check that the choice  $(a_0, b_0) = (a^*, b^*)$  satisfies the condition  $B = 0$ . In other words, the unstable fixed point is part of the separatrix, as it should be.

### APPENDIX C: SPIN-SPIN CORRELATION FUNCTION AT THE CRITICAL POINT: $(1-\gamma)$ -EXPANSION

Here we calculate the spin-spin correlation function

$$\chi_{\text{loc}}(\tau) \equiv \frac{1}{2} \langle T_\tau S^-(\tau) S^+(0) \rangle = \lim_{\lambda \rightarrow \infty} \frac{1}{2} e^{\beta\lambda} \tilde{\chi}, \quad (\text{C1})$$

where  $\tilde{\chi}$  is calculated in the pseudo-fermion representation:

$$\tilde{\chi}(\tau) = \frac{1}{2} \langle T_\tau f_\downarrow^\dagger f_\uparrow(\tau) f_\uparrow^\dagger f_\downarrow(0) \rangle. \quad (\text{C2})$$

It turns out to be convenient to calculate  $\tilde{\chi}$  in terms of

$$G_f^b(\tau) = e^{-\lambda\tau} [(f(\lambda) - 1)\Theta(\tau) + f(\lambda)\Theta(-\tau)]. \quad (\text{C3})$$

The contributions to  $\tilde{\chi}$  are given in Fig. 8. Note that any diagram containing more than one isolated  $f$ -electron bubble vanishes once the limit  $\lambda \rightarrow \infty$  is taken. Fig. 8(a) yields

$$\tilde{\chi}^{(a)}(\tau) = -\frac{1}{2} G_f^b(\tau) G_f^b(-\tau). \quad (\text{C4})$$

In the following, we will restrict  $0 < \tau < \beta$ . Then

$$\tilde{\chi}^{(a)}(\tau) = \frac{1}{2} e^{-\beta\lambda}. \quad (\text{C5})$$

The contribution from Fig. 8(b) is

$$\begin{aligned} \tilde{\chi}^{(b)}(\tau) = & \frac{g^2}{8} \int_0^\beta d\tau_1 \int_0^\beta d\tau_2 G_\phi^b(\tau_1 + \tau_2) \times \\ & \times G_f^b(\tau_1) G_f^b(\tau_2) G_f^b(-\tau_1 - \tau) G_f^b(-\tau_2 + \tau), \end{aligned} \quad (\text{C6})$$

and those from Figs. 8(c) and 8(d) sum to

$$\begin{aligned} \tilde{\chi}^{(cd)}(\tau) = & -\frac{3g^2}{8} \int_0^\beta d\tau_1 \int_0^\beta d\tau_2 G_\phi^b(\tau - \tau_1 - \tau_2) \times \\ & \times G_f^b(\tau_1) G_f^b(\tau_2) G_f^b(\tau - \tau_1 - \tau_2) G_f^b(-\tau) \end{aligned} \quad (\text{C7})$$

Anticipating that  $g^2$  is of order  $1-\gamma$ , to linear order in  $1-\gamma$  we can use Eq. (A4), which corresponds to

$$\begin{aligned} G_\phi^b(\tau) = & \int d\epsilon A_\phi(\epsilon) \frac{1}{\beta} \sum_{i\omega_n} \frac{1}{i\omega_n - \epsilon} e^{-i\omega_n \tau} \\ = & K_0^2 \left( \frac{\pi/\beta}{\sin(\pi\tau/\beta)} \right)^2 \end{aligned} \quad (\text{C8})$$

over the range

$$|\tau| \gg \frac{1}{\Lambda} \quad \text{and} \quad |\beta - \tau| \gg \frac{1}{\Lambda}. \quad (\text{C9})$$

We then have

$$\begin{aligned} \tilde{\chi}^{(b)}(\tau) = & -\frac{g^2}{8} e^{-\beta\lambda} \int_0^{\beta-\tau} d\tau_1 \int_0^\tau d\tau_2 G_\phi^b(\tau_1 + \tau_2) \\ = & -\frac{1}{4} e^{-\beta\lambda} (K_0 g)^2 \ln \left( \frac{\sin(\pi\tau/\beta)}{\pi/\beta\Lambda} \right), \end{aligned} \quad (\text{C10})$$

where the factor  $\Lambda$  appears due to the fact that Eq. (C8) is valid only in the range specified by Eq. (C9). Similarly,

$$\begin{aligned}\tilde{\chi}^{(cd)}(\tau) &= \frac{3g^2}{4} e^{-\beta\lambda} \int_0^\tau d\tau_1 \int_0^{\tau-\tau_1} d\tau_2 G_\phi^b(\tau - \tau_1 - \tau_2) \\ &= -\frac{3}{4} e^{-\beta\lambda} (K_0 g)^2 \ln \left( \frac{\sin(\pi\tau/\beta)}{\pi/\beta\Lambda} \right).\end{aligned}\quad (\text{C11})$$

#### APPENDIX D: LONG-RANGED ONE-DIMENSIONAL SPHERICAL MODEL WITH A LOGARITHMIC-CORRECTION TO ITS RANGE

Consider a spherical model, defined on a chain of  $M$  sites, with a reduced Hamiltonian

$$\mathcal{H}_{sp} = -\frac{1}{2} \sum_{ij} v_{ij} s_i s_j. \quad (\text{D1})$$

Here,  $s_i$  is a scalar variable constrained by the condition

$$\sum_{i=1}^M s_i^2 = M, \quad (\text{D2})$$

with  $M$  being taken to infinity at the end of the calculation. The coupling  $v_{ij}$  represents a long-ranged interaction whose Fourier transform  $v(p) \equiv \sum_j v_{ij} e^{-ipR_{ij}}$  is, for small  $p$ , either

$$v(p) = v - v_1 |p|^x \quad \text{with } 0 < x < 1, \quad (\text{D3})$$

or

$$v(p) = v - \frac{v_1}{\ln(1/|p|)}; \quad (\text{D4})$$

in either case,  $v$  and  $v_1$  are positive constants.

The long-range interaction corresponding to Eq. (D3) has the form

$$v(r) \sim \frac{1}{|r|^{1+x}}. \quad (\text{D5})$$

The solution to this problem is known.<sup>77</sup> An unstable fixed point separates a paramagnetic state from an ordered state. The spin-spin correlation function at the critical point behaves as

$$\chi^{\text{cri}}(r) \sim \frac{1}{|r|^{1-x}}, \quad (\text{D6})$$

while that on the paramagnetic side varies as

$$\chi^{\text{para}}(r) \sim \frac{1}{|r|^{1+x}}. \quad (\text{D7})$$

Eq. (D7) implies that on the paramagnetic side, the exponent of the spin-spin correlation function saturates the bound set by Griffiths' theorem.<sup>52</sup> The result is also

consistent with those for the paramagnetic side of any generic one-dimensional classical spin models with power-law long-ranged interactions.<sup>78–80</sup>

We now consider the problem with a long-range interaction specified by Eq. (D4). In real space,  $v(r)$  has a  $1/|r|$  dependence with a logarithmic correction. We expect that, at the critical point, the spin-spin correlation function should have a pure power-law decay without any logarithmic correction. In the following, we show that this is indeed the case. Standard manipulation<sup>77,81</sup> leads to the following form for the free-energy:

$$F/M = \lambda_0 - \frac{1}{2} \int dp \ln \left( \lambda_0 - v + \frac{v_1}{\ln(1/|p|)} \right), \quad (\text{D8})$$

where the Lagrange multiplier,  $\lambda_0$ , introduced to enforce the constraint, Eq. (D2), is determined by minimizing  $F$ :

$$\frac{1}{2} \int \frac{dp}{\lambda_0 - v + v_1/\ln(1/|p|)} = 1. \quad (\text{D9})$$

The critical point occurs when the solution is such that  $\lambda_0 = v$ , corresponding to

$$\frac{1}{2} \int dp \frac{\ln(1/|p|)}{v_1^c} = 1. \quad (\text{D10})$$

Note that the integral on the left hand side is infrared convergent, establishing the existence of a phase transition. The correlation function at the critical point is given by

$$\chi^{\text{cri}}(p) \sim \frac{1}{v_1^c} \ln \frac{1}{|p|}. \quad (\text{D11})$$

In real space, this corresponds to

$$\chi^{\text{cri}}(r) \sim \frac{1}{|r|} \quad (\text{D12})$$

without any logarithmic correction, which is what we set out to establish.

<sup>1</sup> G. R. Stewart, Rev. Mod. Phys. **73**, 797 (2001).

<sup>2</sup> T. Timusk and B. Statt, Rep. Prog. Phys. **62**, 61 (1999).

<sup>3</sup> C. M. Varma, Z. Nussinov, and W. van Saarloos, Phys. Rep. **361**, 267 (2002).

<sup>4</sup> J. L. Tallon, J. W. Loram, G. V. M. Williams, J. R. Cooper, I. R. Fisher, J. D. Johnson, M. P. Staines, and C. Bernhard, Phys. Stat. Sol. (b) **215**, 531 (1999).

<sup>5</sup> H. v. Löhneysen, T. Pietrus, G. Portisch, H. G. Schlager, A. Schröder, M. Sieck, and T. Trappmann, Phys. Rev. Lett. **72**, 3262 (1994); H. v. Löhneysen, J. Magn. Magn. Mater. **200**, 532 (1999).

<sup>6</sup> N. D. Mathur, F. M. Grosche, S. R. Julian, I. R. Walker, D. M. Freye, R. K. W. Haselwimmer, and G. G. Lonzarich, Nature **394**, 39 (1998); F. M. Grosche, I. R. Walker, S. R. Julian, N. D. Mathur, D. M. Freye, M. J. Steiner, and G. G. Lonzarich, J. Phys.: Condens. Matter **13**, 2845 (2001).

- <sup>7</sup> O. Trovarelli, C. Geibel, S. Mederle, C. Langhammer, F. M. Grosche, P. Gegenwart, M. Lang, G. Sparn, and F. Steglich, *Phys. Rev. Lett.* **85**, 626 (2000).
- <sup>8</sup> K. Heuser, E.-W. Scheidt, T. Schreiner, and G. R. Stewart, *Phys. Rev. B* **57**, R4198 (1998).
- <sup>9</sup> S. Raymond, L. P. Regnault, J. Flouquet, A. Wildes, and P. Lejay, *J. Phys.: Condens. Matter* **13**, 8303 (2001).
- <sup>10</sup> V. A. Sidorov, M. Nicklas, P. G. Pagliuso, J. L. Sarrao, Y. Bang, A. V. Balatsky, and J. D. Thompson, *Phys. Rev. Lett.* **89**, 157004 (2002).
- <sup>11</sup> P. Estrela, A. de Visser, T. Naka, F. R. de Boer, and L. C. J. Pereira, *Eur. Phys. J. B* **23** 449 (2001).
- <sup>12</sup> C. L. Seaman, M. B. Maple, B. W. Lee, S. Ghamaty, M. S. Torikachvili, J.-S. Kang, L. Z. Liu, J. W. Allen, and D. L. Cox, *Phys. Rev. Lett.* **67**, 2882 (1991); M. B. Maple, C. L. Seaman, D. A. Gajewski, Y. Dalichaouch, V. B. Barbetta, M. C. de Andrade, H. A. Mook, H. G. Lukefahr, O. O. Bernal, and D. E. MacLaughlin, *J. Low Temp. Phys.* **95**, 225 (1994).
- <sup>13</sup> B. Andraka and A. M. Tsvetlik, *Phys. Rev. Lett.* **67**, 2886 (1991).
- <sup>14</sup> M. C. Aronson, R. Osborn, R. A. Robinson, J. W. Lynn, R. Chau, C. L. Seaman, and M. B. Maple, *Phys. Rev. Lett.* **75**, 725 (1995).
- <sup>15</sup> O. O. Bernal, D. E. MacLaughlin, H. G. Lukefahr, and B. Andraka, *Phys. Rev. Lett.* **75**, 2023 (1995).
- <sup>16</sup> A. Schröder, G. Aeppli, R. Coldea, M. Adams, O. Stockert, H. v. Löhneysen, E. Bucher, R. Ramazashvili, and P. Coleman, *Nature* **407**, 351 (2000).
- <sup>17</sup> A. Schröder, G. Aeppli, E. Bucher, R. Ramazashvili, and P. Coleman, *Phys. Rev. Lett.* **80**, 5623 (1998).
- <sup>18</sup> O. Stockert, H. v. Löhneysen, A. Rosch, N. Pyka, and M. Loewenhaupt, *Phys. Rev. Lett.* **80**, 5627 (1998).
- <sup>19</sup> A. Rosch, A. Schröder, O. Stockert, and H. v. Löhneysen, *Phys. Rev. Lett.* **79**, 159 (1997).
- <sup>20</sup> J. A. Hertz, *Phys. Rev. B* **14**, 1165 (1976).
- <sup>21</sup> A. J. Millis, *Phys. Rev. B* **48**, 7183 (1993).
- <sup>22</sup> G. G. Lonzarich, in *Electron*, edited by M. Springford (Cambridge Univ. Press, Cambridge, 1997), p. 109.
- <sup>23</sup> T. Moriya, *Spin Fluctuations in Itinerant Electron Magnetism* (Springer, Berlin, 1985); T. Moriya and T. Takimoto, *J. Phys. Soc. Japan* **64**, 960 (1995).
- <sup>24</sup> M. A. Continentino, *Phys. Rev. B* **47**, 11587 (1993).
- <sup>25</sup> M. Lavagna and C. Pépin, *Phys. Rev. B* **62**, 6450 (2000).
- <sup>26</sup> S. Sachdev, *Quantum Phase Transitions* (Cambridge Univ. Press, Cambridge, 1999).
- <sup>27</sup> Q. Si, S. Rabello, K. Ingersent, and J. L. Smith, *Nature* **413**, 804 (2001).
- <sup>28</sup> Q. Si, J. L. Smith, and K. Ingersent, *Int. J. Mod. Phys. B* **13**, 2331 (1999).
- <sup>29</sup> P. Coleman, C. Pépin, and A. M. Tsvetlik, *Phys. Rev. B* **62**, 3852 (2000).
- <sup>30</sup> P. Coleman, *Physica B* **259-261**, 353 (1999).
- <sup>31</sup> A. Rosch, *Phys. Rev. Lett.* **82**, 4280 (1999).
- <sup>32</sup> J. L. Smith and Q. Si, *Phys. Rev. B* **61**, 5184 (2000).
- <sup>33</sup> Q. Si and J. L. Smith, *Phys. Rev. Lett.* **77**, 3391 (1996).
- <sup>34</sup> R. Chitra and G. Kotliar, *Phys. Rev. Lett.* **84**, 3678 (2000).
- <sup>35</sup> S. Doniach, *Physica B* **91**, 231 (1977).
- <sup>36</sup> C. M. Varma, *Rev. Mod. Phys.* **48**, 219 (1976).
- <sup>37</sup> A. Georges, G. Kotliar, W. Krauth, and M. J. Rozenberg, *Rev. Mod. Phys.* **68**, 13 (1996).
- <sup>38</sup> V. N. Popov and S. A. Fedotov, *Sov. Phys. JETP* **67**, 535 (1988).
- <sup>39</sup> J. L. Smith and Q. Si, *cond-mat/9705140*; *Europhys. Lett.* **45**, 228 (1999).
- <sup>40</sup> A. M. Sengupta, *cond-mat/9707316*; *Phys. Rev. B* **61**, 4041 (2000).
- <sup>41</sup> M. Vojta, C. Buragohain, and S. Sachdev, *Phys. Rev. B* **61**, 15152 (2000).
- <sup>42</sup> A. A. Abrikosov, *Physics* **2**, 5 (1965).
- <sup>43</sup> K. G. Wilson and J. Kogut, *Phys. Rep. C* **12**, 75 (1974), especially pp. 133–134.
- <sup>44</sup> A. C. Hewson, *The Kondo Problem to Heavy Fermions* (Cambridge Univ. Press, Cambridge, 1993).
- <sup>45</sup> L. Zhu and Q. Si, *Phys. Rev. B* **66**, 024426 (2002).
- <sup>46</sup> G. Zaránd and E. Demler, *Phys. Rev. B* **66**, 024427 (2002).
- <sup>47</sup> S. Sachdev and J. Ye, *Phys. Rev. Lett.* **70**, 3339 (1993).
- <sup>48</sup> D. R. Grempel and M. J. Rozenberg, *Phys. Rev. Lett.* **80**, 389 (1998).
- <sup>49</sup> O. Parcollet and A. Georges, *Phys. Rev. B* **59**, 5341 (1999).
- <sup>50</sup> D. R. Grempel and Q. Si, *Phys. Rev. Lett.* **91**, 026401 (2003).
- <sup>51</sup> J.-X. Zhu, D. R. Grempel, and Q. Si, *cond-mat/0304033*.
- <sup>52</sup> R. B. Griffiths, *J. Math. Phys.* **8**, 478 (1970).
- <sup>53</sup> For two-dimensional fermions coupled to two-dimensional commensurate spin fluctuations, there are other kinds of singularities in the SDW description; see A. Abanov and A. V. Chubukov, *Phys. Rev. Lett.* **84**, 5608 (2000); A. Abanov, A. V. Chubukov, and J. Schmalian, *Adv. Phys.* **52**, 119 (2003).
- <sup>54</sup> P. Coleman, C. Pépin, Q. Si, and R. Ramazashvili, *J. Phys.: Condens. Matter* **13**, R723 (2001).
- <sup>55</sup> For  $d = z = 2$  the violation of  $\omega/T$  scaling is only logarithmic. A systematic study of these logarithmic terms has recently been reported in S. Pankov, S. Florens, A. Georges, G. Kotliar, and S. Sachdev, *cond-mat/0304415*.
- <sup>56</sup> S. Sachdev and J. Ye, *Phys. Rev. Lett.* **69**, 2411 (1992).
- <sup>57</sup> S. Chakravarty, B. I. Halperin, and D. R. Nelson, *Phys. Rev. B* **39**, 2344 (1989).
- <sup>58</sup> See, for instance, N. Goldenfeld, *Lectures on Phase Transitions and the Renormalization Group* (Addison-Wesley, Reading, 1992).
- <sup>59</sup> P. C. Hohenberg and B. I. Halperin, *Rev. Mod. Phys.* **49**, 435 (1977).
- <sup>60</sup> R. Chitra and Q. Si, unpublished (2000).
- <sup>61</sup> S. Pankov, G. Kotliar, and Y. Motome, *Phys. Rev. B* **66**, 045117 (2002).
- <sup>62</sup> P. Sun and G. Kotliar, *cond-mat/0303539*.
- <sup>63</sup> S. Burdin, M. Grilli, and D. R. Grempel, *Phys. Rev. B* **67**, 121104 (2003).
- <sup>64</sup> E. Miranda, V. Dobrosavljević, and G. Kotliar, *Phys. Rev. Lett.* **78**, 290 (1997).
- <sup>65</sup> A. H. Castro Neto, G. Castilla, and B. A. Jones, *Phys. Rev. Lett.* **81**, 3531 (1998).
- <sup>66</sup> The situation appears to be rather similar to that in the insulating cuprates, where the fluctuations in the paramagnetic phase are essentially two-dimensional (except for intra-unit-cell couplings in bilayered cuprates) but a tiny  $J_{\perp}$  (about  $10^{-5}J_{\parallel}$ ) produces three-dimensional ordering due to a large in-plane correlation length.
- <sup>67</sup> P. Gegenwart, J. Custers, T. Tayama, K. Tenya, C. Geibel, O. Trovarelli, F. Steglich, and K. Neumaier, *Acta Physica*

Polonica B**34**, 323 (2003).

- <sup>68</sup> The Kondo effect inside the ordered phase has been addressed in Ref. 51. Once  $E_{\text{loc}}^*$  vanishes at the QCP it should remain equal to zero inside the antiferromagnetically ordered state. The magnetic ordering removes some spectral weight from the dynamical part of the Weiss field, replacing it by a static Weiss field. Since a static field is more efficient at destroying the Kondo effect than the corresponding dynamical Weiss field, the Kondo effect should remain operative inside the ordered phase.
- <sup>69</sup> A. Yeh, Y.-A. Soh, J. Brooke, G. Aeppli, T. F. Rosenbaum, and S. M. Hayden, *Nature* **419**, 459 (2002).
- <sup>70</sup> R. Hlubina and T. M. Rice, *Phys. Rev. B* **52**, 9253 (1995).
- <sup>71</sup> H. Wilhelm, S. Raymond, D. Jaccard, O. Stockert, H. v. Löhneysen, and A. Rosch, *J. Phys.: Condens. Matter* **13**, L329 (2001).
- <sup>72</sup> F. Steglich, private communications (2002).
- <sup>73</sup> P. W. Anderson, *Phys. Rev.* **124**, 41 (1961).
- <sup>74</sup> S. A. Grigera, R. S. Perry, A. J. Schofield, M. Chiao, S. R. Julian, G. G. Lonzarich, S. I. Ikeda, Y. Maeno, A. J. Millis, and A. P. Mackenzie, *Science* **294**, 329 (2001).
- <sup>75</sup> T. Valla, A. V. Fedorov, P. D. Johnson, B. O. Wells, S. L. Hulbert, Q. Li, G. D. Gu, and N. Koshizuka, *Science* **285**, 2110 (1999).
- <sup>76</sup> G. Aeppli, T. E. Mason, S. M. Hayden, H. A. Mook, and J. Kulda, *Science* **278**, 1432 (1997).
- <sup>77</sup> G. S. Joyce, *Phys. Rev.* **146**, 349 (1966).
- <sup>78</sup> M. E. Fisher, S.-K. Ma, and B. G. Nickel, *Phys. Rev. Lett.* **29**, 917 (1972).
- <sup>79</sup> M. Suzuki, *Prog. Theor. Phys.* **49**, 424, 1106, 1440 (1973).
- <sup>80</sup> J. M. Kosterlitz, *Phys. Rev. Lett.* **76**, 1577 (1976).
- <sup>81</sup> T. H. Berlin and M. Kac, *Phys. Rev.* **86**, 821 (1952).
- <sup>82</sup> I. S. Gradshteyn and I. M. Ryzhik, *Tables of Integrals, Series, and Products*, 5<sup>th</sup> Edition (Academic Press, 1994), Section 2.211.